https://doi.org/10.1093/plcell/koad030 THE PLANT CELL 2023: 35: 1408–1428

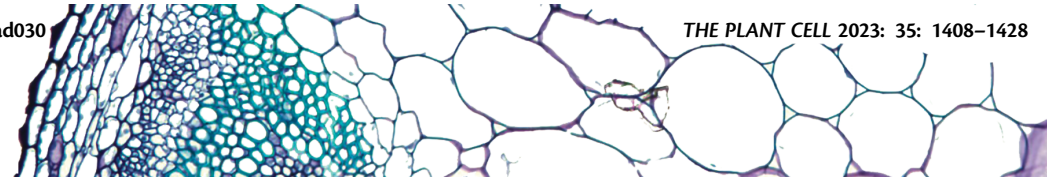

Research Article

Proteasomal degradation of MaMYB60 mediated by the E3 ligase MaBAH1 causes high temperature-induced repression of chlorophyll catabolism and green ripening in banana

Wei Wei [1], Ying-ying Yang [1], Prakash Lakshmanan [2,3,4], Jian-fei Kuang [1], Wang-jin Lu [1], Xue-qun Pang [5], Jian-ye Chen [1,*] and Wei Shan [1,*]

1 State Key Laboratory for Conservation and Utilization of Subtropical Agro-bioresources/Guangdong Provincial Key Laboratory of Postharvest Science of Fruits and Vegetables/Engineering Research Center of Southern Horticultural Products Preservation, Ministry of Education, College of Horticulture, South China Agricultural University, Guangzhou 510642, China
2 Sugarcane Research Institute, Key Laboratory of Sugarcane Biotechnology and Genetic Improvement (Guangxi), Ministry of Agriculture/ Guangxi Key Laboratory of Sugarcane Genetic Improvement, Guangxi Academy of Agricultural Sciences, Nanning 530007, China
3 Interdisciplinary Research Center for Agriculture Green Development in Yangtze River Basin, Southwest University, Chongqing 400716, China
4 Queensland Alliance for Agriculture and Food Innovation, University of Queensland, St Lucia, QLD 4067, Australia
5 College of Life Sciences, South China Agricultural University, Guangzhou 510642, China

*Author for correspondence: chenjianye@scau.edu.cn (J.-y.C), shanwei@scau.edu.cn (W.S.)

Abstract

Banana (*Musa acuminata*) fruits ripening at 30 °C or above fail to develop yellow peels; this phenomenon, called green ripening, greatly reduces their marketability. The regulatory mechanism underpinning high temperature-induced green ripening remains unknown. Here we decoded a transcriptional and post-translational regulatory module that causes green ripening in banana. Banana fruits ripening at 30 °C showed greatly reduced expression of 5 chlorophyll catabolic genes (CCGs), *MaNYC1* (*NONYELLOW COLORING 1*), *MaPPH* (*PHEOPHYTINASE*), *MaTIC55* (*TRANSLOCON AT THE INNER ENVELOPE MEMBRANE OF CHLOROPLASTS 55*), *MaSGR1* (*STAY-GREEN 1*), and *MaSGR2* (*STAY-GREEN 2*), compared to those ripening at 20 °C. We identified a MYB transcription factor, MaMYB60, that activated the expression of all 5 CCGs by directly binding to their promoters during banana ripening at 20 °C, while showing a weaker activation at 30 °C. At high temperatures, MaMYB60 was degraded. We discovered a RING-type E3 ligase MaBAH1 (benzoic acid hypersensitive 1) that ubiquitinated MaMYB60 during green ripening and targeted it for proteasomal degradation. MaBAH1 thus facilitated MaMYB60 degradation and attenuated MaMYB60-induced transactivation of CCGs and chlorophyll degradation. By contrast, MaMYB60 upregulation increased CCG expression, accelerated chlorophyll degradation, and mitigated green ripening. Collectively, our findings unravel a dynamic, temperature-responsive MaBAH1–MaMYB60–CCG module that regulates chlorophyll catabolism, and the molecular mechanism underpinning green ripening in banana. This study also advances our understanding of plant responses to high-temperature stress.

Introduction

The visual appearance of fruits, particularly their color, is an important quality attribute for fruit dealers and consumers. Fruit color is affected by environmental factors such as temperature, light, nutrients, drought, and salinity (Santos 2004; Momose and Ozeki 2013; Lee et al. 2014; Rolando et al. 2015). The recurring and more frequent incidence of high temperatures in the tropics is becoming a major threat

Received December 19, 2022. Accepted January 16, 2023. Advance access publication February 7, 2023

to fruit yield and product quality. Banana (*Musa acuminata*, AAA group), the most popular fresh fruit consumed worldwide, are harvested at the mature-green stage and ripened to a golden yellow peel with ethylene (Kuang et al. 2017; Xiao et al. 2018).

During banana ripening, the temperature is the crucial element affecting fruit quality formation. Ripening at temperatures above 24 °C (e.g. 30 °C) makes fruits soften faster but reduces yellowing, and the peel remains fully green. This phenomenon, called green ripening, is highly undesirable and causes losses in fruit quality for banana marketing. Previous studies detected an association between green ripening and lack of chlorophyll degradation, lipid loss, and sugar accumulation in the peel (Blackbourn et al. 1990; Drury et al. 1999; Yang et al. 2009; Du et al. 2014). By contrast, rapid chlorophyll degradation and peel color change occur in many other fruits such as tomato (*Solanum lycopersicum*) and citrus (*Citrus* spp.) at higher temperatures (Ogura et al. 1975; Cohen 1978). Given the adverse commercial impact of green ripening in banana and because it starts appearing at a moderately high temperature, understanding the molecular regulation of high temperature-induced loss of chlorophyll degradation in ripening bananas will help to develop technological solutions to this problem, which may be aggravated by global warming.

Chlorophyll catabolism is largely controlled via the transcriptional modulation of genes encoding the enzymes involved in leaf senescence and fruit ripening. Many chlorophyll catabolic genes (CCGs) have been identified and characterized, forming a complete enzymatic reaction system for chlorophyll degradation; these genes include *NONYELLOW COLORING 1* (*NYC1*, encoding a chlorophyll *b* reductase), *7-HYDROXYMETHYL CHLOROPHYLL A (HMCHL) REDUCTASE* (*HCAR*), *STAY-GREEN*s (*SGR*s, encoding Mg-dechelatases), *PHEOPHYTINASE* (*PPH*), *PHEOPHORBIDE A OXYGENASE* (*PAO*), *RED CHLOROPHYLL CATABOLITE REDUCTASE* (*RCCR*), and *TRANSLOCON AT THE INNER ENVELOPE MEMBRANE OF CHLOROPLASTS 55* (*TIC55*, encoding a C32 hydroxylase) (Pružinská et al. 2003; Guo et al. 2004; Meguro et al. 2011; Christ et al. 2016; Hauenstein et al. 2016; Shimoda et al. 2016; Zhang et al. 2016; Kuai et al. 2018).

Our understanding of the genetic regulators and regulatory mechanism(s) involved in chlorophyll degradation during fruit maturation and post-harvest ripening is expanding. For instance, silencing of the NAC (NAM, ATAF1/2, CUC) transcription factor *SlNAC4* in tomato fruits downregulated several CCGs and repressed chlorophyll breakdown during maturation (Zhu et al. 2014). Similarly, another tomato NAC transcription factor, nonripening-like 1 (NOR-like 1), directly binds to the promoter of *SlSGR1*, enhancing its transcription during fruit ripening; fruits from mutants in *NOR-like1* fail to turn fully red and remain orange until the final ripe stage (Gao et al. 2018). In citrus fruit, ethylene-response factor 6 (CitERF6) and CitERF13 induce *CitPPH* and accelerate chlorophyll degradation (Yin et al. 2016; Li et al. 2019a). More notably, comparative transcriptomic and proteomic analyses of banana fruits stored at 20 °C or 30 °C revealed significant downregulation of several CCGs and chlorophyll catabolic enzymes at 30 °C, which was well correlated with repressed chlorophyll degradation at high temperatures (Du et al. 2016; Li et al. 2019b). However, the molecular regulation of these CCGs under high temperatures, repressing chlorophyll catabolism and causing green ripening in banana, remains unknown.

In fruits, MYB transcription factors have been implicated as crucial regulators of color formation (Dubos et al. 2010; Xu et al. 2015). For instance, SlMYB12 increases naringenin chalcone production, and its downregulation leads to the formation of pink tomato fruit (Adato et al. 2009). In apples (*Malus domestica*), MdMYB1 regulates anthocyanin biosynthesis and transport during fruit color development (Li et al. 2012; Jiang et al. 2019), and MdMYB10 controls flesh color by activating *dihydroflavonol 4-reductase* (*MdDFR*) expression through its interaction with MdbHLH3 and MdbHLH33 (Espley et al. 2007; Rihani et al. 2017). MYBs are also involved in carotenoid and chlorophyll accumulation. In a stay-green mutant of *Citrus reticulata* cv Suavissima, CrMYB68 negatively regulated the carotenoid biosynthetic gene *β-carotene hydroxylase 2* (*CrBCH2*) (Zhu et al. 2017). AdMYB7 in kiwifruit (*Actinidia deliciosa*) and SlMYB72 in tomato activate key chlorophyll biosynthesis genes to modulate chlorophyll accumulation and chloroplast development (Ampomah-Dwamena et al. 2019; Wu et al. 2020).

Emerging evidence suggests that turnover of MYB proteins is regulated by post-translational modifications such as ubiquitination (Lee and Seo 2016; Millard et al. 2019; Wang et al. 2021). Interestingly, under normal ambient temperature (~22 °C), MYB15 inhibits the expression of *C-repeat/DRE binding factor*s (*CBF*s) to facilitate normal plant growth and development. However, when plants are exposed to cold stress, 2 U-box type E3 ubiquitin ligases, Plant U-Box 25 (PUB25) and PUB26, poly-ubiquitinate and degrade MYB15, leading to the activation of the CBF-dependent cold signaling pathway (Wang et al. 2019). However, whether MYBs are targets of ubiquitination under high temperatures and subsequently affect high temperature-associated physiology needs to be elucidated.

Here, we explored this question as part of our research on the molecular mechanism(s) of high temperature-induced inhibition of chlorophyll degradation in banana fruits, a phenomenon opposite to what normally occurs in other tissues such as leaves exposed to high temperature. During the green ripening of banana fruits at 30 °C, 5 CCGs (*MaNYC1*, *MaSGR1*, *MaSGR2*, *MaPPH*, and *MaTIC55*) were downregulated and chlorophyll degradation was inhibited. We demonstrate here that a MYB transcription factor, MaMYB60, targeted and activated these 5 CCGs and accelerated chlorophyll degradation. Conversely, *MaMYB60* overexpression attenuated high temperature-induced repression of chlorophyll catabolism. Importantly, we identified the RING-type E3 ligase benzoic acid hypersensitive 1 (MaBAH1) as interacting with and ubiquitinating MaMYB60, causing its degradation via the 26S

proteasome pathway. Furthermore, the MaBAH1-mediated degradation of MaMYB60 was enhanced under high temperatures, which decreased MaMYB60-promoted chlorophyll degradation. Together, these key findings unravel an important regulatory module for chlorophyll degradation, and explain the molecular basis of green ripening in banana.

Results

Altered gene expression of 5 CCGs is important for high temperature-induced green ripening in bananas

To explore the effect of high temperature on chlorophyll degradation in peels during banana fruit ripening, we compared ripening progression of bananas under 20 °C and 30 °C. The peels of banana fruits ripened at 20 °C turned yellow 2 d after ethylene treatment, and completely de-greened by Day 5. However, bananas ripened at 30 °C remained green even on Day 6, reflecting the high retention of chlorophyll in the peel (Fig. 1A). The change in peel color patterns was associated with a rapid increase in the color index (CI) in fruit ripened at 20 °C compared to that at 30 °C (Fig. 1B). Consistent with the CI change, total chlorophyll content also declined at both temperatures, but the rate of decline was greater at 20 °C than at 30 °C. By Day 6, ∼78.0% of the chlorophyll was degraded in bananas kept at 20 °C compared to ∼34.0% in fruits ripened at 30 °C (Fig. 1C). Thus, the green ripening banana fruits is associated with the repression of chlorophyll catabolism.

To unravel the molecular regulators and the regulatory mechanism repressing chlorophyll degradation during banana ripening under high temperatures, we conducted a systematic, detailed molecular study of green ripening. We first analyzed the expression of 9 CCGs involved in chlorophyll catabolism: *MaNYC1*, *NYC1-LIKE* (*MaNOL*), *MaHCAR*, *MaSGR1*, *MaSGR2*, *MaPPH*, *MaPAO*, *MaRCCR*, and *MaTIC55*, in the peels of bananas stored at 20 °C and 30 °C by reverse-transcription quantitative PCR (RT-qPCR). The transcripts of *MaNYC1*, *MaSGR1*, *MaSGR2*, *MaPPH*, and *MaTIC55* became abundant following ethylene treatment in bananas ripening at 20 °C, whereas those of *MaPAO* and *MaNOL* decreased, and those of *MaRCCR* and *MaHCAR* displayed no obvious change (Fig. 1D). By contrast, the expression levels of *MaNYC1*, *MaSGR1*, *MaSGR2*, *MaPPH*, and *MaTIC55* were significantly lower in fruits kept at 30 °C throughout the entire ripening progression (Fig. 1D). However, the transcript levels of *MaRCCR* increased more at 30 °C than at 20 °C, but those of *MaNOL*, *MaHCAR*, and *MaPAO* displayed no consistent differences between the 2 treatments (Fig. 1D).

To identify the most important changes in CCG expression associated with green ripening, we analyzed the expression levels of all 9 CCGs by the variable importance in projection (VIP) method combined with partial least squares-discriminant analysis (PLS-DA), which is a supervised multivariate approach widely used to identify key genes and metabolites that contribute to changes in transcriptome and metabolome analyses (Papazian et al. 2016). As shown in the PLS-DA model, CCG expression profiles in fruits ripened at 30 °C clearly deviated from those ripened at 20 °C (Supplemental Fig. S1A), with *MaSGR2* making the most significant contribution to the model, as evidenced by its highest VIP score (Supplemental Fig. S1B), followed by *MaSGR1*, *MaNYC1*, *MaRCCR*, *MaTIC55*, and *MaPPH*, with the last 3 genes making a relatively smaller contribution.

Transient overexpression in *Nicotiana benthamiana* leaves is an effective method that is widely used for evaluating the biological function of genes, including CCGs (Xiang et al. 2019). We thus transiently individually overexpressed *MaNYC1*, *MaSGR1*, *MaSGR2*, *MaPPH*, or *MaTIC55* in *N. benthamiana* leaves to examine their potential ability to mediate chlorophyll degradation. We determined that all 5 CCGs have a positive effect on chlorophyll degradation, with *MaSGR2* showing the best ability to induce yellowing, as indicated by chlorophyll fluorescence imaging of F_v/F_m (maximum potential quantum efficiency of photosystem II) and Y(II) (actual photosynthetic efficiency), and a significant decrease in total chlorophyll content (Supplemental Fig. S2, A–C). These data indicate that these 5 CCGs, whose expression was repressed by high temperature, and particularly *MaSGR2*, might be important candidate genes for chlorophyll degradation in banana fruits, and thus they were selected for further experiments.

Identification of MaMYB60, a transcriptional activator of CCGs in banana fruit

To identify the upstream regulators of *MaSGR2*, we cloned the *MaSGR2* promoter and looked for proteins that bind to its sequence in a yeast one-hybrid (Y1H) screen using a cDNA library prepared from ripening banana peels. In this screen, we identified a MYB family transcription factor, designated MaMYB60 (Ma04_g00460). We confirmed the interaction between MaMYB60 and the *MaSGR2* promoter using the full-length coding sequence of *MaMYB60* as prey in the Y1H assay. As shown in Fig. 2A, we detected no basal activity from the *MaSGR2* promoter driving the reporter of the assay in the presence of aureobasidin A (AbA), whereas yeast cells expressing *MaMYB60* induced the expression of the AbA resistance gene driven by the *MaSGR2* promoter and grew well on medium containing AbA, verifying that MaMYB60 binds to the *MaSGR2* promoter.

We also characterized the molecular properties of MaMYB60. Phylogenetic analysis indicated that MaMYB60 is most closely related to Arabidopsis (*Arabidopsis thaliana*) MYB60 (Supplemental Fig. S3A), and contains both the R2 and R3 DNA-binding domains (Supplemental Fig. S3B) that recognize MYB recognition sequences (MYBRs) in the promoters of target genes (Prouse and Campbell 2012). Consistent with a role of a transcription factor, a subcellular localization assay showed that a MaMYB60-GFP (green fluorescent protein) fusion protein localized to the nucleus when the encoding construct was transiently expressed in

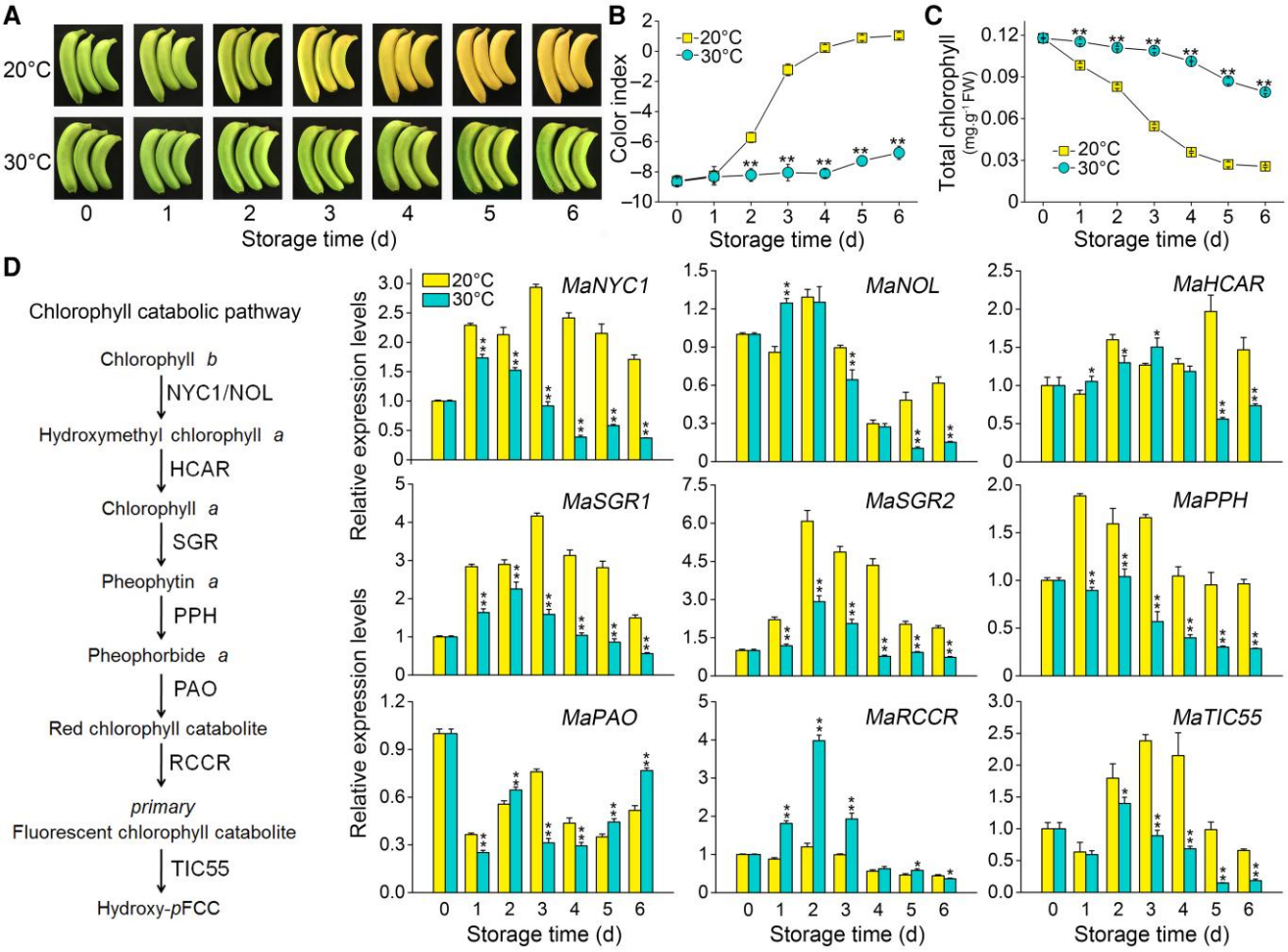

Figure 1. Chlorophyll degradation and expression of 9 CCGs during banana fruit ripening at 20 °C and 30 °C. A) Appearance of banana peel during ripening at 20 °C and 30 °C. B, C) Changes in CI B) and total chlorophyll contents C) during fruit ripening. D) Expression of 9 CCGs (*MaNYC1*, *MaNOL*, *MaHCAR*, *MaSGR1*, *MaSGR2*, *MaPPH*, *MaPAO*, *MaRCCR*, and *MaTIC55*) in banana peel during fruit ripening. The chlorophyll catabolic pathway is represented to the left, with the RT-qPCR data shown to the right. Expression levels were normalized to values on Day 0, which were set to 1. Data are means ± SE from $n = 6$ B, C) and $n = 3$ D) biological replicates. Asterisks highlight significant differences in banana peel at 30 °C compared to 20 °C as determined by Student's *t*-test, $^{*}P < 0.05$ and $^{**}P < 0.01$.

N. benthamiana leaf epidermal cells (Supplemental Fig. S4B). Moreover, MaMYB60 exhibited transcriptional activation activity through its C-terminal region (domain 1.2), in a Y1H assay and in plants in a dual-luciferase reporter assay when fused to the yeast GAL4 DNA-binding domain (Supplemental Fig. S4, C and D).

To test whether MaMYB60 directly binds to the promoter of *MaSGR2* and the other 4 CCGs, we isolated their respective promoters and identified their putative MYBRs (Supplemental Fig. S5). We then performed an electrophoretic mobility shift assay (EMSA), which showed that purified recombinant glutathione S-transferase (GST)-MaMYB60 (Supplemental Fig. S4A) can bind directly to MYBRs-containing fragments derived from each of these 5 promoters and caused clear mobility shifts (Fig. 2, B–F). Moreover, the shifted bands disappeared upon the addition of increasing amounts of unlabeled wild-type probes, but not by mutated probes. We independently confirmed the binding of MaMYB60 to these promoters by chromatin immunoprecipitation (ChIP)-qPCR. As shown in Fig. 2G, an anti-MaMYB60 antibody pulled down the proximal promoter regions of these 5 CCGs, but we detected no significant ChIP signals over the distal promoter regions.

We also tested whether MaMYB60 can activate the transcription of these 5 CCGs in a transient dual-luciferase-based transactivation assay. To this end, we placed the firefly luciferase (*LUC*) reporter gene under the control of each promoter individually and co-infiltrated each with a construct overexpressing *MaMYB60* as effector. As shown in Fig. 2H, the activities of the *MaNYC1*, *MaSGR1*, *MaSGR2*, *MaPPH*, and *MaTIC55* promoters were greatly enhanced in the presence of MaMYB60, with a considerably higher LUC/Renilla luciferase (REN) ratio compared to that of the control.

Together, these data indicate that MaMYB60 acts as a transcriptional activator of CCG (*MaNYC1*, *MaSGR1*, *MaSGR2*, *MaPPH*, and *MaTIC55*) transcription by directly targeting their promoters.

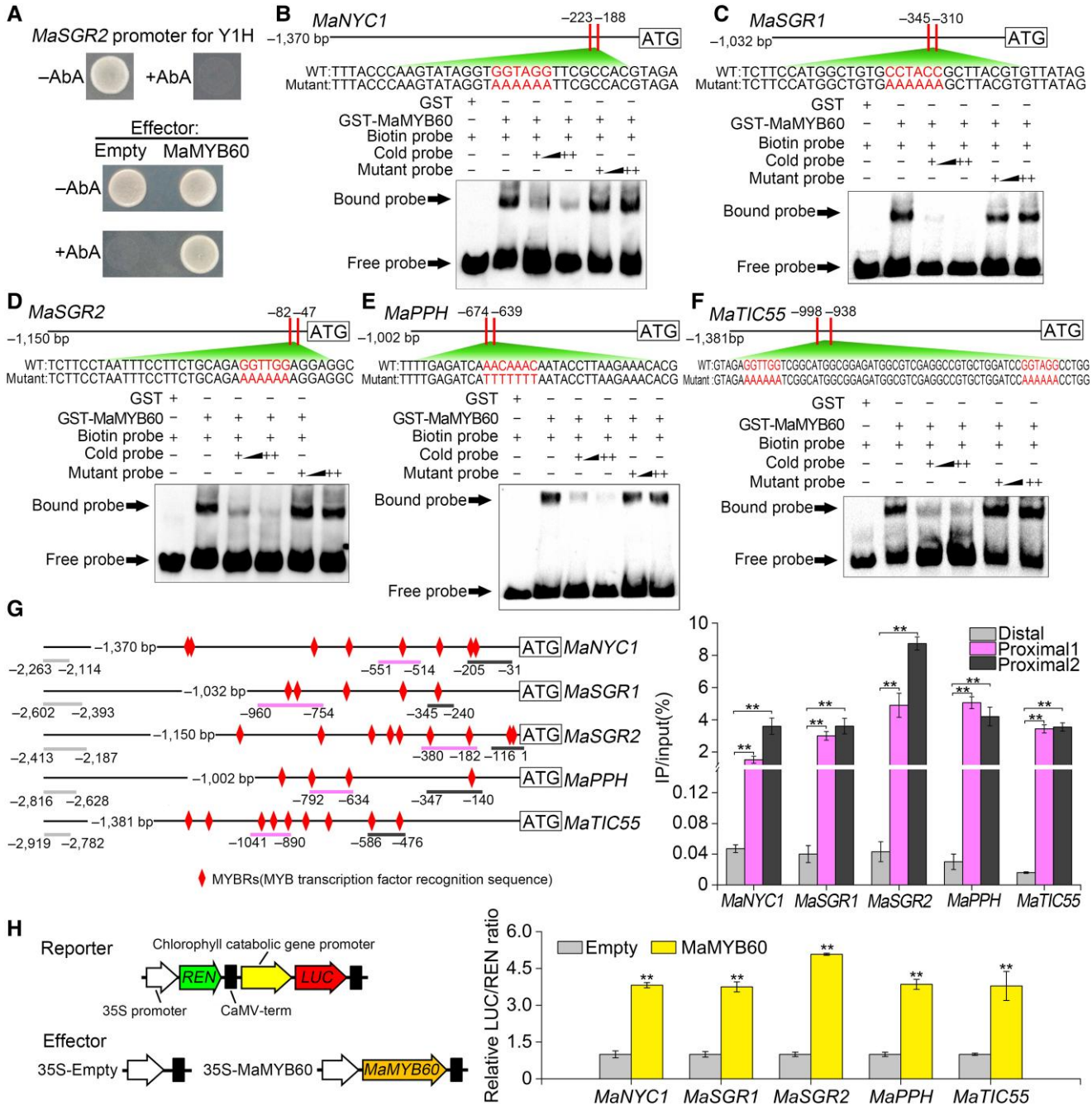

Figure 2. MaMYB60 activates the expression of 5 CCGs by directly binding to their promoters. A) Physical interaction of MaMYB60 with the *MaSGR2* promoter in a Y1H assay. Top, No basal expression of the *MaSGR2* promoter was detected in yeast grown on synthetic defined (SD) medium lacking Leu in the presence of 300 ng mL^{-1} AbA. Bottom, Yeast growth assay after the Y1H reporter strain was transformed with plasmids expressing *MaMYB60* or empty (pGADT7, negative control). B–F) EMSA showing the in vitro binding of recombinant MaMYB60 to the promoters of *MaNYC1* B), *MaSGR1* C), *MaSGR2* D), *MaPPH* E), and *MaTIC55* F). The wild type (WT) and mutant probe sequences for each CCG promoter are shown at the top of the image. Recombinant GST (negative control) or GST-MaMYB60 was incubated with each probe, followed by separation on native poly-acrylamide gels. Triangles indicate increasing amounts of unlabeled intact or mutated probes for competition. G) ChIP-qPCR assay showing the in vivo binding of MaMYB60 to the CCG promoters. Left, schematic representation of each CCG promoter structure. MYBR and probes used for ChIP-qPCR assay are indicated with red diamonds, black (proximal 1), and red (proximal 2) underlines, respectively. The distal promoter region indicated by white underlines was used as negative control. Right, ChIP-qPCR results. Values are the percentage of DNA samples immunoprecipitated with the anti-MaMYB60 antibody relative to input DNA. H) Transactivation of *MaNYC1*, *MaSGR1*, *MaSGR2*, *MaPPH*, and *MaTIC55* promoters by MaMYB60. Left, schematic diagrams of reporter and effector vectors. Right, relative luciferase activity values. LUC/REN from the empty vector plus promoter–reporter were set to 1. Data are means ± SE from $n = 3$ G) or $n = 6$ H) biological replicates. Student's *t*-test, $^{**}P < 0.01$.

MaMYB60 promotes chlorophyll catabolism and attenuates high temperature-induced repression of chlorophyll degradation

We performed a set of experiments to test the role of MaMYB60 in mediating chlorophyll catabolism. Transient overexpression of *MaMYB60* in *N. benthamiana* leaves led to a remarkable yellowing around the infiltration site (Supplemental Fig. S6A), which was characterized by significant chlorophyll loss and a significant decrease in F_v/F_m, Y(II) compared to empty control (Supplemental Fig. S6, B and C). In parallel, endogenous *N. benthamiana* CCGs (*NbNYC1*, *NbSGR1*, *NbSGR2*, *NbPPH*, and *NbTIC55*) displayed significantly higher transcript levels in leaves infiltrated with *MaMYB60* relative to the empty vector control (Supplemental Fig. S6D). We subsequently examined the function of MaMYB60 in banana fruits through transient silencing and overexpression. A comparison of *MaMYB60*-silenced fruit with the control established that knockdown of endogenous *MaMYB60* transcripts hindered chlorophyll degradation and led to a green phenotype near the injection point (Fig. 3, A and B). Concomitantly, we measured a lower CI and higher chlorophyll contents (Fig. 3C), as well as the downregulation of all 5 banana CCGs (*MaNYC1*, *MaSGR1*, *MaSGR2*, *MaPPH*, and *MaTIC55*) (Fig. 3D), in the *MaMYB60*-silenced area. Conversely, transient overexpression of *MaMYB60* promoted chlorophyll degradation at 30 °C, resulting in a distinct de-greening phenotype around the injection site (Fig. 3, E and F), which was supported by the higher CI, lower chlorophyll content (Fig. 3G), and upregulated CCG expression (Fig. 3H).

We validated the biological function of MaMYB60 by its stable overexpression in Arabidopsis. In *MaMYB60* -overexpressing lines (*MaMYB60*-OE-1, -2, and -3), leaves turned yellow faster than in WT during senescence (Supplemental Fig. S7, A and B). Accordingly, *MaMYB60*-OE plants had lower chlorophyll contents and higher expression levels of Arabidopsis CCGs (*AtNYC1*, *AtSGR1*, *AtSGR2*, *AtPPH*, and *AtTIC55*) than the nontransgenic control (Supplemental Fig. S7, C and D).

Collectively, these results indicate that MaMYB60 acts as a positive regulator of chlorophyll degradation, and its overexpression attenuates the high-temperature-repressed chlorophyll catabolism by enhancing CCG expression.

High temperature induces the proteasomal degradation of MaMYB60

To elucidate how high temperate represses MaMYB60-activated chlorophyll catabolism, we examined *MaMYB60* expression and MaMYB60 abundance in banana peels at 20 °C and 30 °C. *MaMYB60* transcript levels were markedly lower in the fruits ripened at 30 °C compared to those at 20 °C on Days 3, 4, and 6 of storage (Fig. 4A). Interestingly, immunoblotting analysis showed that MaMYB60 abundance significantly decreased at 30 °C at all time points, using a specific antibody raised against MaMYB60 for this study (Fig. 4B). Compared to *MaMYB60* transcript abundance, MaMYB60 protein levels showed a higher correlation coefficient with CI, chlorophyll content, and CCG transcript levels (Fig. 4C and Supplemental Figs. S8 and S9). With this result, we investigated the effect of ambient temperature on MaMYB60 protein stability.

Ubiquitin-proteasome system-mediated proteolysis occurs in all eukaryotic cells (Kerscher et al. 2006). To determine whether MaMYB60 is a target for proteasomal degradation, we analyzed MaMYB60 abundance in bananas treated with the proteasomal inhibitor MG132 and incubated at 20 °C or 30 °C, using the anti-MaMYB60 antibody. As shown in Fig. 4D, pretreatment with MG132 maintained high levels of MaMYB60 protein at 30 °C but had no obvious effect on the already high protein abundance at 20 °C (Fig. 4D). Furthermore, a ChIP-qPCR assay of peels from green bananas ripened at 30 °C indicated a lower binding for MaMYB60 to the CCG promoters, compared to that in bananas ripened at 20 °C. This inhibition, however, was attenuated to a considerable extent by MG132 treatment (Fig. 4E). These results suggest that high temperature induces MaMYB60 protein degradation via the proteasome pathway, and thereby attenuates the MaMYB60 transactivation of CCGs.

The RING-type E3 ligase MaBAH1 interacts with MaMYB60

Proteasome-mediated protein degradation requires ubiquitin E3 ligase-mediated ubiquitination. To identify the E3 ligase that is responsible for the high temperature-induced proteasomal degradation of MaMYB60, we performed immunoprecipitation followed by mass spectrometry (IP-MS) to investigate the protein-interacting partners of MaMYB60 (Supplemental Fig. S10A). Interestingly, we identified a RING-type E3 ubiquitin ligase (Ma05_p02600), a candidate protein that may interact with MaMYB60 (Supplemental Fig. S10B and Supplemental Data Set S1). This protein has significant sequence similarity with Arabidopsis BAH1, which is characterized by the presence of an SPX (SYG1/Pho81/XPR1) domain and a C3HC4-type RING finger domain (Supplemental Figs. S10 and S11); hence we designated this protein as MaBAH1.

We validated the interaction between MaMYB60 and MaBAH1 by yeast two-hybrid (Y2H) assay. As shown in Fig. 5A, yeast cells co-transformed with *MaMYB60* and *MaBAH1* turned blue in the presence of the chromogenic substrate α-Gal, as did the positive control, while the negative controls did not, indicating that MaMYB60 interacts with MaBAH1 in yeast cells. An in vitro GST pull-down assay indicated that recombinant GST-MaMYB60, but not GST alone, can be pulled down by maltose-binding protein (MBP)-MaBAH1 (Fig. 5B). A co-localization assay showed that although we detected MaBAH1 in the nucleus, cytoplasm, and plasma membrane, MaBAH1 co-localized with MaMYB60 in the nucleus (Fig. 5C), suggesting the possible interaction between these 2 proteins in planta. Subsequently, we confirmed their interaction in living plant cells by split-luciferase assay and co-immunoprecipitation

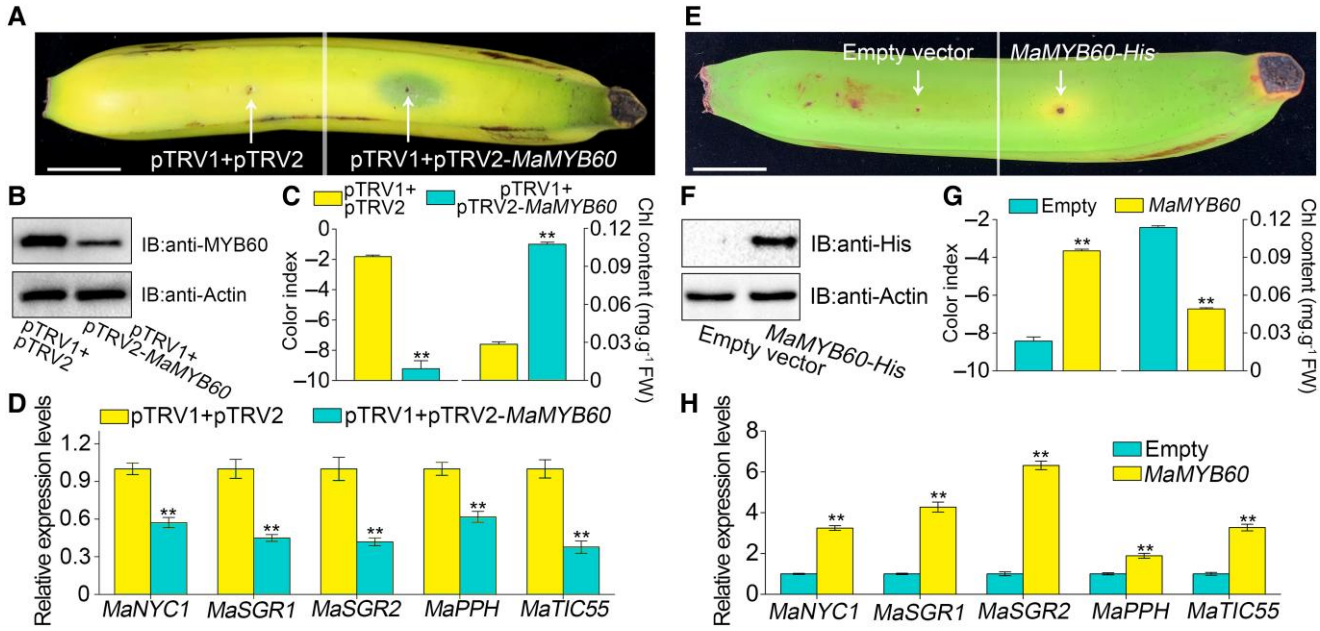

Figure 3. MaMYB60 promotes chlorophyll degradation and weakens the inhibition of chlorophyll catabolism at high temperature. A–D) Transient silencing of *MaMYB60* in banana fruits inhibits chlorophyll degradation. A) Appearance of banana fruit infiltrated with empty vector (left side of fruit peel) and pTRV2-*MaMYB60* (right) at 3 d after ethylene treatment. Scale bar, 2 cm. B) Immunoblotting of MaMYB60 in the infiltrated banana peel. Fruit peel tissues at the injection region were used for immunoblotting, using Actin as loading control. C) Changes in the CI and total chlorophyll content of banana peels as shown in A). D) CCG expression in banana peels as shown in A). E–H) Transient overexpression of *MaMYB60* in banana fruit weakens high temperature-inhibiting chlorophyll catabolism. E) Appearance of bananas infiltrated with empty vector (left side of peel) and *MaMYB60-His* (right) at 3 d under 30 °C. F) Immunoblotting detection of MaMYB60-His in banana peels infiltrated with empty vector or *MaMYB60-His*. Fruit peel tissues at the injection region were used for protein detection with an anti-His monoclonal antibody, using Actin as loading control. G) Changes in the CI and total chlorophyll content in peels as shown in E). H) Expression of *MaNYC1*, *MaSGR1*, *MaSGR2*, *MaPPH*, and *MaTIC55* in peels as shown in E). Data are means ± SE with $n = 6$ C, G) or $n = 3$ D, H) biological replicates. Asterisks indicate significant differences, as determined by Student's *t*-test, $^{**}P < 0.01$.

(Co-IP). In the split-luciferase assay, we detected the activity from reconstituted luciferase in *N. benthamiana* leaves co-expressing *MaMYB60-NLUC* (encoding MaMYB60 fused to the N-terminal half of LUC) and *CLUC-MaBAH1* (encoding the C-terminal half of LUC fused to MaMYB60). However, we detected no LUC activity in the negative control combinations (Fig. 5D). In the Co-IP assay, MaMYB60-GFP immunoprecipitated MaBAH1-His, but not GFP, when using an anti-GFP antibody for IP (Fig. 5E). Overall, these data demonstrate the in vitro and in vivo interaction of MaMYB60 with MaBAH1.

MaBAH1 ubiquitinates MaMYB60 for proteasomal degradation

Given that MaBAH1 has E3 ubiquitin ligase activity (Supplemental Fig. S12) and interacts with MaMYB60 (Fig. 5), we assessed whether MaBAH1 can ubiquitinate MaMYB60 through an in vitro ubiquitination assay using purified recombinant GST-MaMYB60 along with MBP-MaBAH1. After co-incubation of GST-MaMYB60 and MBP-MaBAH1 in the presence of ubiquitin, an E1 ubiquitin-activating enzyme and an E2 ubiquitin-conjugating enzyme, we observed the ubiquitination of GST-MaMYB60, as indicated by the higher molecular weight bands in this sample alone (Fig. 6A). However, we detected no ubiquitinated signal when any one of these components in the reaction was missing (Fig. 6A). We also tested the ubiquitination of MaMYB60 by MaBAH1 in vivo via co-expression of *MaMYB60-GFP* and *MaBAH1-His* constructs in *N. benthamiana* leaves. As shown in Fig. 6B, after immunoprecipitation of MaMYB60-GFP with anti-GFP beads, we used an anti-Ub antibody to detect poly-ubiquitinated MaMYB60, which was present in significantly higher quantities when *MaMYB60-GFP* was co-expressed with *MaBAH1-His* than with the empty-His control vector, indicating that MaBAH1 can promote MaMYB60 ubiquitination.

To validate whether MaBAH1 mediates the degradation of MaMYB60, we conducted a cell-free degradation assay. To this end, we incubated purified recombinant GST-MaMYB60 with equal amounts of total proteins extracted from *N. benthamiana* leaves transiently expressing *MaBAH1-His* or the empty-His vector control. Immunoblotting analysis showed that the GST-MaMYB60 protein is degraded more rapidly in the protein extracts expressing *MaBAH1-His* than in those expressing empty-His (Fig. 6C). To further examine whether MaBAH1 mediates the degradation of MaMYB60 through the 26S proteasome pathway, we transiently expressed

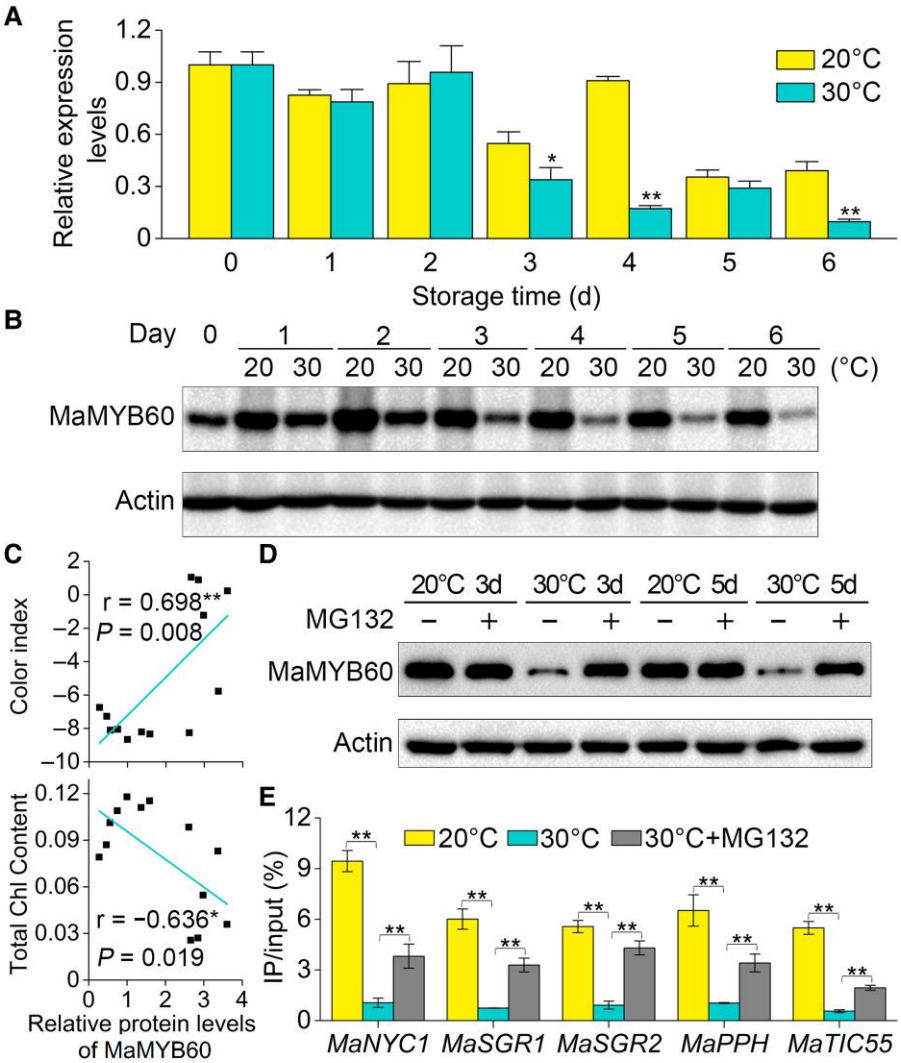

Figure 4. High temperature induces proteasomal degradation of MaMYB60 and reduces its binding to CCG promoters. A) Changes in *MaMYB60* transcript levels in banana fruits during ripening at 30 °C or 20 °C. Expression levels were normalized to values on Day 0, which were set to 1. Data are means ± SE from 3 biological replicates. Asterisks indicate significant differences between banana peel at 30 °C and 20 °C as determined by Student's *t*-test: $^{*}P < 0.05$ and $^{**}P < 0.01$. B) Changes in MaMYB60 abundance at 30 °C and 20 °C. An equal amount of total protein (30 μg) per lane was subjected to SDS–PAGE, followed by immunoblotting using the anti-MaMYB60 antibody, with Actin as loading control. C) Correlation between MaMYB60 protein levels and CI and total chlorophyll content. Relative MaMYB60 abundance was measured using ImageJ software; the correlation coefficients were calculated by SPSS Statistics 20. Asterisks indicate significant differences as determined by Student's *t*-test, $^{*}P < 0.05$ and $^{**}P < 0.01$. D) Immunoblotting assay of MaMYB60 in bananas treated with the proteasomal inhibitor MG132 at 20 °C and 30 °C. Actin was used as loading control. E) ChIP-qPCR assay of MaMYB60 binding activity to the promoters of CCGs (*MaNYC1*, *MaSGR1*, *MaSGR2*, *MaPPH*, and *MaTIC55*) at 30 °C and 20 °C. Data are means ± SE from 3 biological replicates, Student's *t*-test, $^{**}P < 0.01$.

MaMYB60-LUC and *MaBAH1* in *N. benthamiana* leaves. Immunoblotting analysis with an anti-LUC antibody revealed that MaMYB60 abundance declined substantially in the presence of MaBAH1, compared to the empty vector control, and this decline was inhibited by MG132 (Fig. 6D). Quantification of LUC activity also showed that the presence of MaBAH1 caused MaMYB60 protein degradation, while the addition of MG132 in the reaction mixture abolished this response (Fig. 6E). These results demonstrate that MaBAH1 ubiquitinates MaMYB60 and facilitates its degradation via the 26S proteasome pathway.

High temperature enhances MaBAH1 mediated-proteasomal degradation of MaMYB60

We then asked whether MaBAH1 mediated-proteasomal degradation of MaMYB60 is affected by high temperature. Quantitative analyses of RNA and protein levels in fruits ripened at 20 °C or 30 °C showed increased levels of *MaBAH1* mRNA and MaBAH1 protein in the peels of fruits incubated at 30 °C as compared to those kept at 20 °C (Fig. 7A and Supplemental Fig. S13). The protein level of MaMYB60 was negatively correlated with that of MaBAH1, with $R = -0.573$ ($P < 0.05$) (Fig. 7B). Moreover, a Co-IP assay

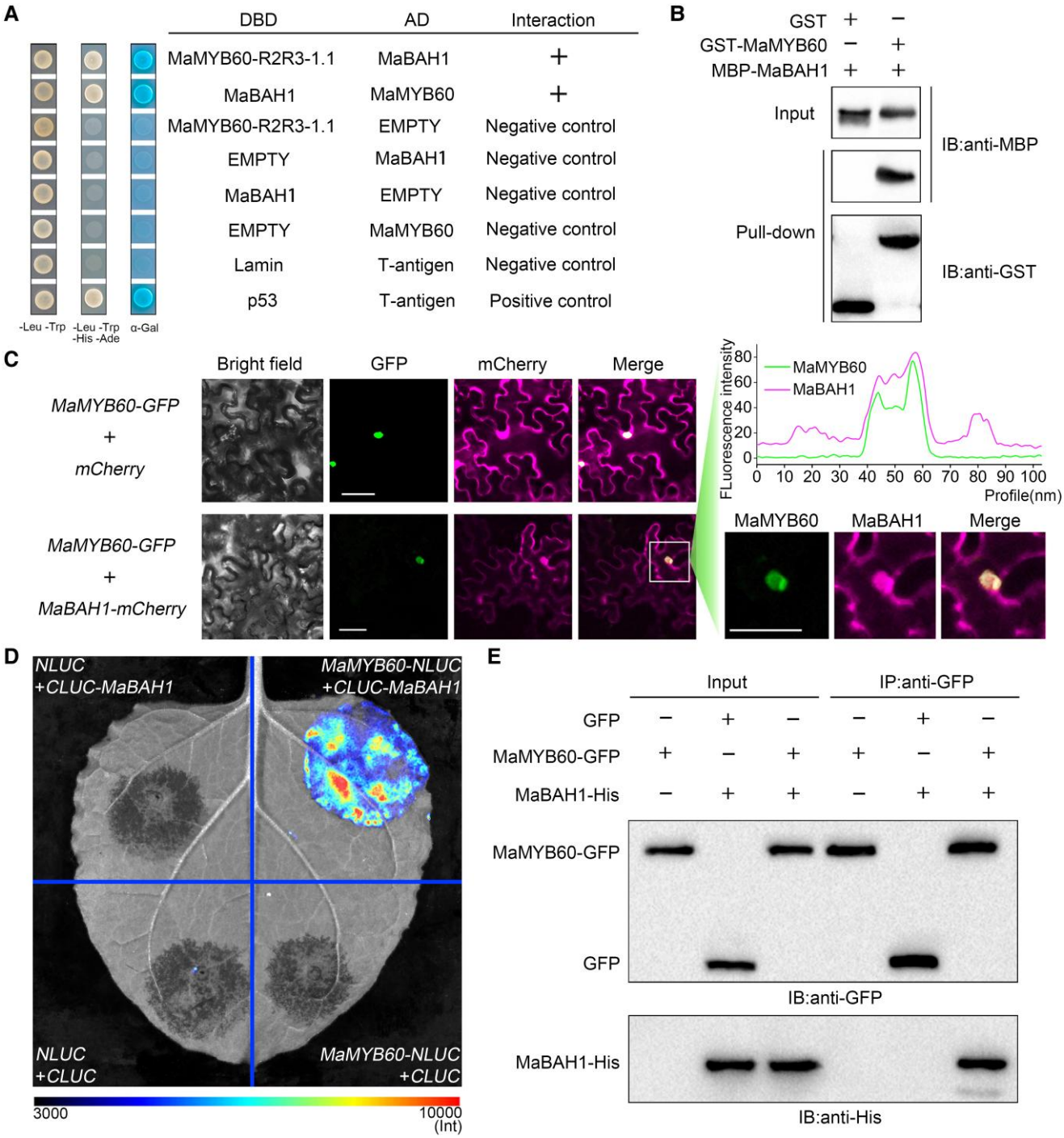

Figure 5. MaBAH1 physically interacts with MaMYB60. A) Y2H assay showing the interaction between MaBAH1 and MaMYB60. Yeast cells co-transformed with *DBD-MaMYB60-R2R3-1.1* and *AD-MaBAH1*, or *DBD-MaBAH1* and *AD-MaMYB60*, were grown on SD medium (lacking Trp, Leu, His and Ade) in the presence of the chromogenic substrate α-Gal. B) In vitro GST pull-down assay showing the interaction of MaBAH1 with MaMYB60. Recombinant MBP-MaBAH1 was incubated with GST-MaMYB60 or GST, the bound proteins were then detected by immunoblotting using anti-MBP or anti-GST antibodies, respectively. C) Co-localization analysis of MaMYB60-GFP and MaBAH1-mCherry. *MaMYB60-GFP* was co-expressed with *MaBAH1-mCherry* or *mCherry* in *N. benthamiana* leaves via Agrobacterium-mediated infiltration. The boxed region is enlarged at the right. The graph above shows the co-localization analysis using fluorescence-intensity profiles for GFP and mCherry signals. Scale bars, 25 μm. D) Split-luciferase assay in *N. benthamiana* leaves showing the interaction between MaMYB60 and MaBAH1. *MaMYB60-NLUC* was co-expressed with *CLUC-MaBAH1*; *MaMYB60-NLUC/CLUC*, *NLUC/CLUC-MaBAH1*, and *NLUC/CLUC* were used as negative controls. Luciferase activity was recorded with a CCD camera. Representative images of *N. benthamiana* leaves at 72 h after infiltration are shown. E) In vivo Co-IP assay showing the interaction of MaMYB60 with MaBAH1. *MaMYB60-GFP* and *MaBAH1-His*, *GFP* and *MaBAH1-His*, or *MaMYB60-GFP* alone, were transiently expressed in *N. benthamiana* leaves and immunoprecipitated with an anti-GFP antibody. Immunoprecipitated samples and input controls were detected with anti-GFP and anti-His antibodies, respectively.

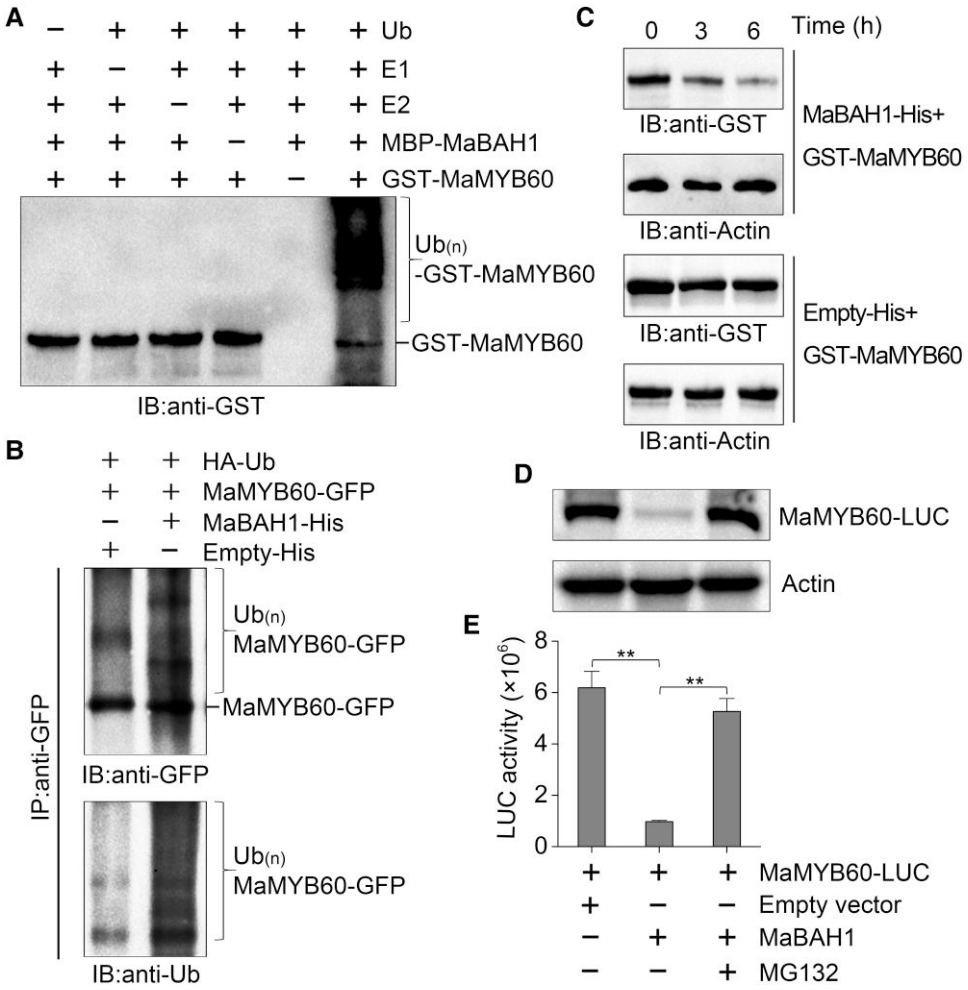

Figure 6. MaBAH1 mediates MaMYB60 protein degradation via the ubiquitin–proteasome system. A) MaBAH1 ubiquitinates MaMYB60 in vitro. The activity of recombinant MBP-BAH1 in GST-MaMYB60 ubiquitynation was tested in the presence and absence of ubiquitin, E1, E2, MBP-BAH1, and GST-MaMYB60. Ubiquitynated GST-MaMYB60 was detected by immunoblotting with an anti-GST antibody. B) In vivo ubiquitination of MaMYB60 by MaBAH1. Ubiquitynated proteins in total protein extracts from *N. benthamiana* leaves transiently expressing *HA-Ub*, *MaMYB60-GFP* and *MaBAH1-His* or Empty-His in different combinations, were captured with anti-GFP antibody. Ubiquitynated MaMYB60 was detected using anti-GFP and anti-ubiquitin antibodies. C) Cell-free degradation assay of recombinant GST-MaMYB60. Protein extracts from *N. benthamiana* leaves transiently expressing *MaBAH1-His* or empty-His vector were, respectively, incubated with recombinant GST-MaMYB60 for the indicated times. GST-MaMYB60 protein levels were determined using anti-GST antibody, with Actin as loading control. D, E) Proteasome-mediated degradation assay of MaMYB60 in plant cells. *MaMYB60-LUC* was co-expressed with *MaBAH1* or empty vector in *N. benthamiana* leaves in the presence or absence of MG132. D) Abundance of MaMYB60 as analyzed by immunoblotting using an anti-LUC antibody, with Actin as loading control. E) Stability of MaMYB60, as indicated by measuring luciferase activity. Data are means ± SE from 6 biological replicates. Asterisks indicate significant differences as determined by Student's *t*-test (**$P < 0.01$).

using an anti-MaMYB60 antibody on total proteins extracted from banana peel showed a higher amount of high-molecular mass forms of MaMYB60 corresponding to poly-ubiquitinated MaMYB60 (Ubi(n)-MaMYB60) in the peels of banana fruits ripened at 30 °C than those at 20 °C, as evidenced by immunoblotting with an anti-Ub antibody (Fig. 7C). Further, we observed a decrease in MaMYB60 abundance and an increase in MaBAH1 protein levels in the samples immunoprecipitated with the anti-MaMYB60 from banana fruits ripened at 30 °C compared to those at 20 °C (Fig. 7C). These results suggest that MaBAH1 mediated-proteasomal degradation of MaMYB60 is temperature-dependent and is stimulated under high temperatures.

MaBAH1 attenuates MaMYB60 activation of CCGs and chlorophyll degradation

Because MaBAH1 mediated the ubiquitination and degradation of MaMYB60, we hypothesized that MaBAH1 might interfere with the MaMYB60-mediated transactivation of CCGs. We tested this hypothesis by performing transient overexpression assays in *N. benthamiana* leaves using the

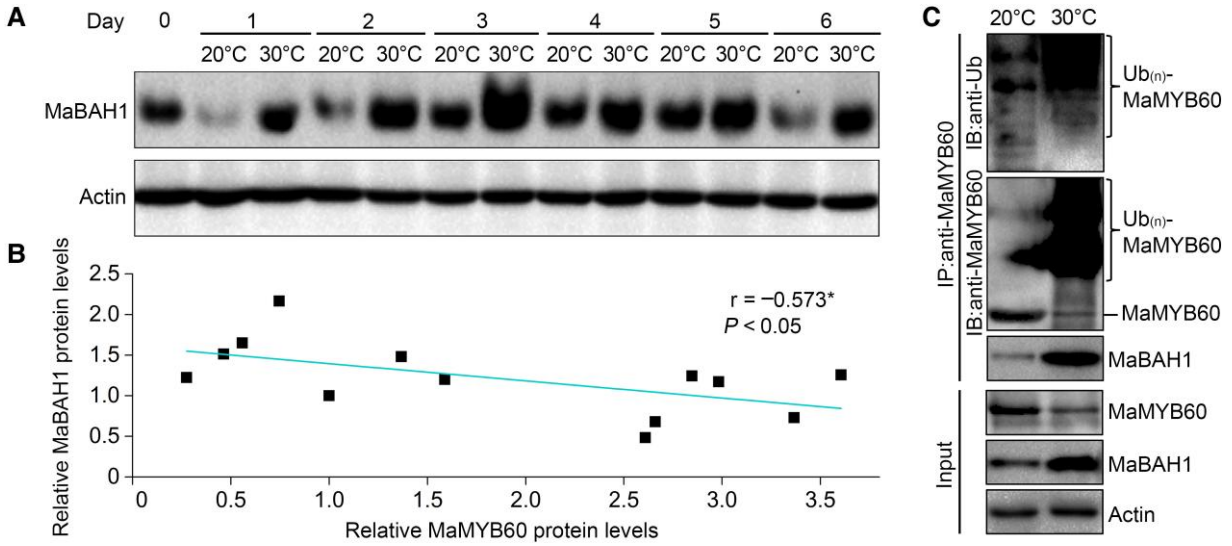

Figure 7. MaBAH1 is involved in high temperature-induced ubiquitination and degradation of MaMYB60. A) Changes in MaBAH1 protein accumulation in banana fruit during ripening at 30 °C and 20 °C. An equal amount of total protein (30 μg) per lane from each time point sample was subjected to immunoblotting using the anti-MaBAH1 antibody, with Actin as loading control. B) MaBAH1 and MaMYB60 protein levels are correlated, based on quantification from immunoblotting by densitometric analysis using ImageJ software. Asterisks indicate significant differences as determined by Student's *t*-test (*$P < 0.05$). C) MaBAH1 participates in high temperature-promoted ubiquitination of MaMYB60. MaMYB60 in the total protein extracted from banana fruit ripened at 30 °C and 20 °C was immunoprecipitated with the anti-MaMYB60 antibody. Ubiquitinated MaMYB60 was detected using anti-ubiquitin and anti-MaMYB60 antibodies. The presence of MaBAH1 in the immunoprecipitated complex was determined using an anti-MaBAH1 antibody, with Actin as loading control.

dual-luciferase reporter system. Compared to the empty vector control, the expression of *MaMYB60* activated *LUC* transcription from the *MaNYC1*, *MaSGR1*, *MaSGR2*, *MaPPH*, and *MaTIC55* promoters, and this activation was attenuated when MaBAH1 was present (Fig. 8A). However, the MaBAH1-mediated repression of CCG transactivation by MaMYB60 was largely eliminated when MG132 was included in the reaction mixture (Fig. 8A).

We further asked whether MaMYB60-induced chlorophyll degradation was inhibited by MaBAH1 via transiently overexpressing *MaBAH1* and *MaMYB60* in *N. benthamiana* leaves (Supplemental Fig. S14A). Transient overexpression of MaMYB60 caused distinct yellowing of leaves and considerable chlorophyll loss with a significant decrease in F_v/F_m and Y(II), while co-expression with *MaBAH1* rescued the phenotype substantially (Supplemental Fig. S14B). Consistent with this observation, overexpression of *MaMYB60* resulted in lower total chlorophyll contents and induced the expression of *N. benthamiana* CCGs (*NbNYC1*, *NbSGR1*, *NbSGR2*, *NbPPH*, and *NbTIC55*), while this induction was repressed in the presence of MaBAH1 (Supplemental Fig. S14, C and D). Notably, the addition of MG132 largely eliminated the effect of MaBAH1 and maintained MaMYB60-induced chlorophyll degradation (Supplemental Fig. S14, B–D).

To validate the MaBAH1-mediated repression of chlorophyll degradation in bananas, we conducted transiently silenced and overexpressed *MaBAH1* in banana fruits. As shown in Fig. 8B, the transient overexpression of *MaBAH1* in banana peels led to a green phenotype near the injection point, in contrast to the yellow phenotype at the empty vector-injected site. We detected lower levels of MaMYB60 in *MaBAH1*-overexpressing tissues (Fig. 8C). In parallel, we observed a lower CI and measured higher chlorophyll contents in the *MaBAH1*-injected area (Fig. 8D), as well as decreased CCG expression (Fig. 8E). By contrast, *MaBAH1* silencing increased MaMYB60 protein levels and caused a distinct de-greening phenotype near the vector injection point at high temperature, compared to the area that received the empty control vector (Fig. 8, F and G). Consistent with this observation, we measured an increased CI, decreased total chlorophyll contents (Fig. 8H), and increased expression of CCGs (Fig. 8I) in *MaBAH1*-silenced tissues. In addition, the stable heterologous expression of *MaBAH1* in Arabidopsis delayed leaf yellowing, which was accompanied by high chlorophyll contents and lower expression of CCGs (Supplemental Fig. S15). Thus, our data establish that MaBAH1 attenuates the MaMYB60-mediated activation of CCGs and contributes to high temperature-inhibited chlorophyll catabolism through the proteasomal degradation of MaMYB60.

Discussion

De-greening, caused by rapid chlorophyll degradation, is a normal phenomenon associated with leaf senescence and ripening of most fruits. Since maintaining chlorophyll extends the time for fixed carbon assimilation and grain development, the stay-green trait has been investigated in many

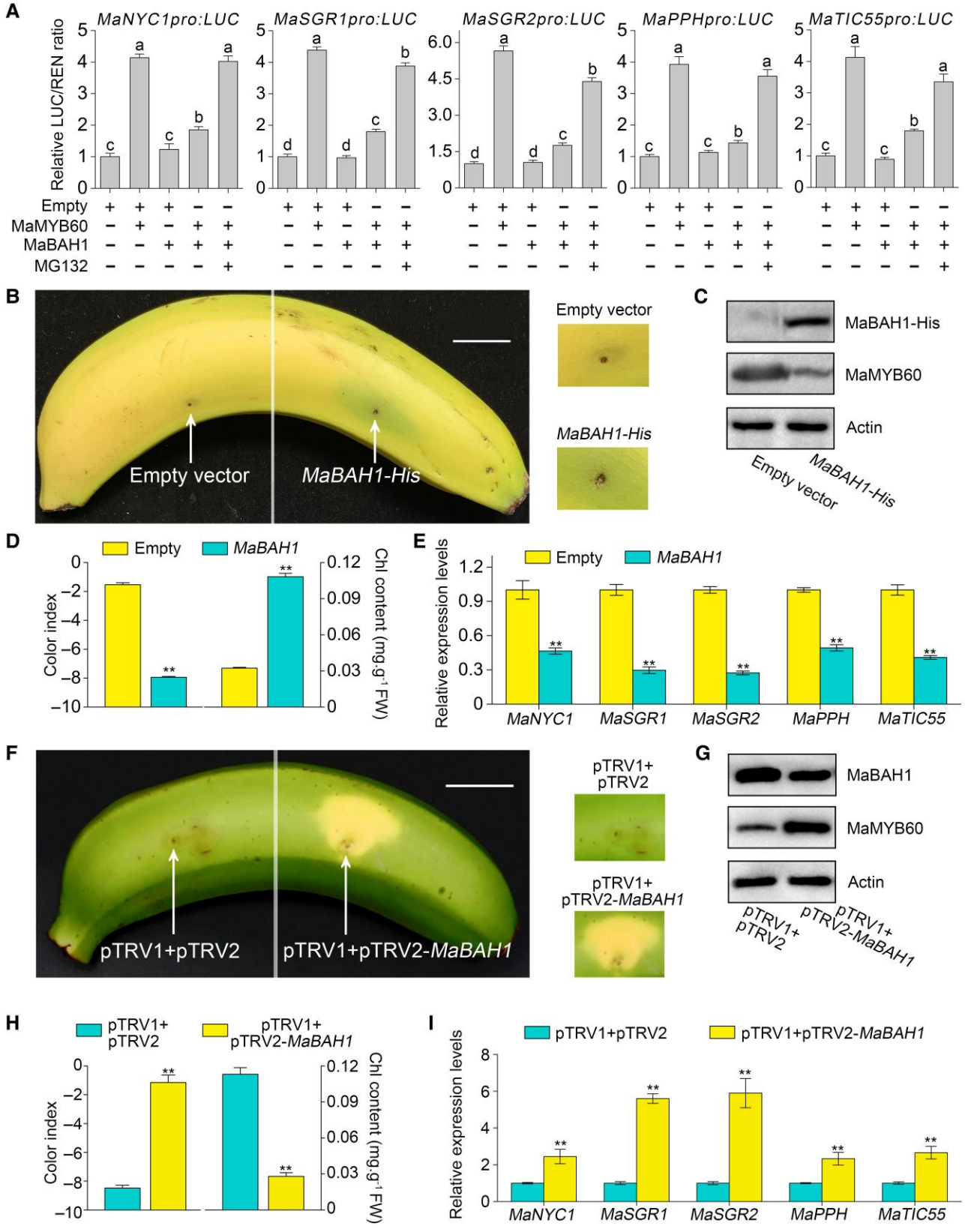

Figure 8. Attenuation of MaMYB60-induced chlorophyll degradation by MaBAH1. A) MaBAH1 suppresses MaMYB60-mediated transactivation of the *MaNYC1*, *MaSGR1*, *MaSGR2*, *MaPPH*, and *MaTIC55* promoters. *LUC* driven by CCG promoters (*MaNYC1pro:LUC*, *MaSGR1pro:LUC*, *MaSGR2pro:LUC*, *MaPPHpro:LUC*, and *MaTIC55pr:LUC*) and *REN* driven by the CaMV 35S promoter (as an internal control) in the same vector, we co-expressed

(continued)

crops including rice (*Oryza sativa*; Cha et al. 2002), wheat (*Triticum aestivum*; Rampino et al. 2006), soybean (*Glycine max*; Fang et al. 2014), barley (*Hordeum vulgare*; Gous et al. 2017), and tomato (Barry et al. 2008), and the trait is now a target for plant breeding. With climate change and the global warming-associated reduction in agricultural productivity, the stay-green trait appears to be effective in improving heat resistance (Abdelrahman et al. 2017; Kamal et al. 2019). In most cases, heat stress promotes chlorophyll degradation and causes chlorophyll contents to decrease (Wang et al. 2018; Janni et al. 2020). However, it can be delayed remarkably or abolished completely in some cases, such as in banana fruit (Thomas and Howarth 2000). In Cavendish-type bananas, which dominate the world market, fruit ripening at or above 24 °C suppresses chlorophyll degradation (Yang et al. 2009). Noticeably, the temperature range at which green ripening occurs is not high enough to inhibit enzymatic reactions. These facts suggest that temperature-dependent inhibition of chlorophyll degradation in banana fruits may be regulated by an unknown temperature-regulated chlorophyll degradation mechanism, which our findings elucidate. This new knowledge offers opportunities for innovations in banana fruit post-harvest technology and the development of cultivars that do not undergo green ripening under high temperatures.

During leaf senescence, the expression of CCGs is directly regulated by multiple transcription factors (Qiu et al. 2015; Gao et al. 2016; Chen et al. 2017; Kuai et al. 2018). However, less attention has been given to the transcriptional regulation of CCGs during fruit ripening. MYB transcription factors function as upstream regulators of carotenoid, anthocyanin and chlorophyll biosynthesis, and contribute to fruit color formation (Rihani et al. 2017; Zhu et al. 2017; Ampomah-Dwamena et al. 2019; Jiang et al. 2019; Wu et al. 2020), while direct evidence for the regulation of chlorophyll catabolism by MYBs is still lacking. In this study, we showed that high temperature reduced the expression of *MaNYC1*, *MaSGR1*, *MaSGR2*, *MaPPH*, and *MaTIC55*, resulting in the repression of chlorophyll degradation in green ripening bananas (Fig. 1). We identified the MYB protein MaMYB60 that bound directly to the promoters of *MaNYC1*, *MaSGR1*, *MaSGR2*, *MaPPH*, and *MaTIC55*, and positively regulated their expression (Fig. 2). Overexpression of *MaMYB60* decreased chlorophyll content in *N. benthamiana* and Arabidopsis leaves, and banana fruit peels, while *MaMYB60*-silencing hindered chlorophyll degradation (Fig. 3; Supplemental Figs. S6 and S7). These findings demonstrate that MaMYB60 positively regulates chlorophyll degradation in bananas by directly activating CCGs.

Interestingly, the transient overexpression of *MaMYB60* in banana peels attenuated the inhibition of chlorophyll degradation by high temperatures (Fig. 3, E–H). This result suggests that the repression of MaMYB60-induced chlorophyll degradation at 30 °C, i.e. is green ripening, may be mediated by some unknown mechanism. Both *MaMYB60* mRNA and MaMYB60 protein levels were lower at 30 °C than at 22 °C, while MaMYB60 protein levels were more correlated with the green ripening phenotype (Fig. 4 and Supplemental Figs. S8 and S9). In addition, we detected *MaMYB60* transcript and MaMYB60 protein at high levels in banana fruits, compared to their levels in roots, stems, and leaves (Supplemental Fig. S16), suggesting that MaMYB60 exerts its actions mainly in the fruit. Ubiquitination is an important post-translational modification affecting protein stability, thus playing key regulatory roles in various biological decisions including temperature-stress responses (Wang et al. 2019). Our current results showed that banana ripening at 30 °C induced MaMYB60 degradation via the proteasome pathway, which in turn abolished MaMYB60 activation of CCGs (Fig. 4, D and E). Moreover, MG132 treatments only partially rescued the binding and activation of CCGs by MaMYB60, suggesting that both the transcriptional and post-translational regulation of MaMYB60 play a role in chlorophyll degradation during green ripening.

In apple fruits, MdMYB23 and MdMYB308L, which regulate cold tolerance and anthocyanidin accumulation, are ubiquitinated and degraded by the BTB (BROAD-COMPLEX, TRAMTRACK, AND BRIC A BRAC2) protein MdBT2 and the RING E3 ligase MdMIEL1 (MYB30-Interacting E3 Ligase 1), respectively (An et al. 2018, 2020, 2021). In our study, we identified the high temperature-inducible RING-type ubiquitin E3 ligase MaBAH1 as a MaMYB60-interacting protein that promoted the ubiquitination-mediated proteasomal degradation of MaMYB60, and functioned as a negative regulator of chlorophyll degradation (Figs. 5–8 and Supplemental Figs. S14 and S15). In an apparent contradiction of our

(**Figure 8.** Continued)
with an effector plasmid expressing *MaMYB60* or *MaBAH1* in *N. benthamiana* leaves. The LUC/REN ratio of the empty vector + CCG*pro:LUC* reporter was set to 1. Data are means ± SE from 6 biological replicates. Different lowercase letters indicate significant differences as determined by one-way ANOVA followed by Tukey's test ($P < 0.05$). B–E) Transient overexpression of *MaBAH1* in banana fruit inhibits chlorophyll degradation. B) Appearance of banana fruit injected with empty vector (left side of peel) and *MaBAH1-His* (right) at 3 d after ethylene treatment. Scale bar: 2 cm. C) Immunoblotting analysis of banana peel injected with empty vector and *MaBAH1-His*. MaBAH1 and MaMYB60 were detected with anti-His and anti-MaMYB60 antibodies, respectively, with Actin as loading control. D) Changes in the CI and total chlorophyll content in bananas peels as shown in B). E) Expression of CCGs in banana peels as shown in B). F–I) Transient silencing of *MaBAH1* in banana fruits weakens high temperature-induced inhibition of chlorophyll catabolism. F) Appearance of banana fruit injected with empty vector (left side of peel) and pTRV2-*MaBAH1* (right) at 3 d under 30 °C. Scale bar: 2 cm. G) Immunoblotting of MaBAH1 in injected banana peel. Actin served as loading control. H) Changes in the CI and total chlorophyll content in banana peels as shown in F). I) CCG expression in banana peels as shown in F). Data are means ± SE from $n = 6$ D, H) and $n = 3$ E, I) biological replicates. Asterisks indicate significant differences as determined by Student's *t*-test (**$P < 0.01$).

results, a recent report in apple described how the ethylene-activated E3 ubiquitin ligase MdPUB24 promoted chlorophyll degradation by the degradation of BEL1-LIKE HOMEODOMAIN transcription factor 7 (MdBEL7), leading to the enhanced expression of CCGs (*CHLOROPHYLLASE* [*MdCLH*], *MdPPH2*, and *CAROTENOID AND CHLOROPLAST REGULATION 2* [*MdRCCR2*]) (Wei et al. 2021). Here, it is important to note that our work clearly demonstrated the enhancement of MaBAH1-mediated ubiquitination and proteasomal degradation of MaMYB60 under high temperatures (Fig. 7). Our data also established that high-temperature suppressed MaMYB60-induced chlorophyll degradation by activating MaBAH1-mediated proteasomal degradation of MaMYB60, thus unraveling a new molecular regulatory module controlling chlorophyll catabolism under heat stress. In Arabidopsis, the RING finger ubiquitin E3 ligase, HIGH EXPRESSION OF OSMOTICALLY RESPONSIVE GENES 1 (HOS1), interacts with and ubiquitinates INDUCER OF CBF EXPRESSION 1 (ICE1), leading to ICE1 degradation and thus preventing CBF-induced expression of COLD-REGULATED (*COR*) genes (Dong et al. 2006). In another example, PUB25 and PUB26, 2 U-box type E3 ubiquitin ligases, trigger MYB15 degradation through the ubiquitin-proteosome pathway, thereby enhancing cold-induced *CBF* gene expression and plant cold tolerance (Wang et al. 2019). Collectively, E3 ligase-mediated proteasomal degradation may be widespread in plant responses to temperature stress, including both low-temperature and high-temperature stresses, thereby enabling plant adaptation under extreme temperature conditions.

Interestingly, despite the fact that low temperature induces PUB25- and PUB26-mediated degradation of MYB15, overexpression of *MYB15* results in reduced cold tolerance in Arabidopsis (Agarwal et al. 2006; Kim et al. 2017; Wang et al. 2019). Similarly, overexpression of *MaMYB60* accelerated chlorophyll degradation in bananas under high temperatures (Fig. 3, E–H), even if MaMYB60 had undergone MaBAH1-mediated degradation in this condition (Fig. 7). These results suggest the existence of a threshold beyond which high temperature-induced proteasomal degradation of transcription factors may be deficient. Several pieces of evidence lead us to speculate that this threshold might be determined by the activity of E3 ligase. For instance, the kinase OPEN STOMATA 1 (OST1) phosphorylates PUB25 and PUB26 and stimulates their E3 activities, which in turn enhances cold-induced degradation of MYB15 (Wang et al. 2019). Additionally, ICE1 is phosphorylated by protein kinases to prevent its interaction with E3 ligases, which thus enhances its protein stability, indicating that phosphorylation antagonizes ubiquitination to maintain substrate protein stability (Ding et al. 2015; Zhang et al. 2017). E3 ligases are also targeted by other E3 ubiquitin ligases for proteasomal degradation, which affects the functional activity of the initial E3 ligase as well. For example, the Arabidopsis E3 ligase SALT- AND DROUGHT-INDUCED RING FINGER 1 (SDIR1) degrades EIN3-BINDING F BOX PROTEIN 1 (EBF1) and EBF2, which in turn disables EBF1/EBF2 to degrade ETHYLENE-INSENSITIVE3 (EIN3), thereby fine-tuning the ethylene response to fluctuating ambient temperatures (Hao et al. 2021). These results suggest the regulatory roles of phosphorylation and ubiquitination crosstalk in dynamically and precisely regulating plant responses to temperature stresses. Thus, it will be of considerable interest to investigate whether another E3 ligase or protein kinase affects the regulation of MaMYB60 by MaBAH1 under high temperatures.

Based on our findings, we propose a working model depicting the molecular basis of high temperature-induced repression of chlorophyll degradation causing green ripening in bananas (Fig. 9). During banana fruit ripening at 20 °C, MaMYB60 directly targets and activates the expression of CCGs, including *MaNYC1*, *MaSGR1*, *MaSGR2*, *MaPPH*, and *MaTIC55*, leading to chlorophyll degradation and yellowing of banana peel. When bananas ripen at 30 °C, the elevated temperature enhances *MaBAH1* expression and MaBAH1 abundance. MaBAH1 interacts with and ubiquitinates MaMYB60, resulting in MaMYB60 proteasomal degradation and the repression of the MaMYB60-mediated induction of CCGs, causing green ripening in banana. Taken together, our findings establish a regulatory module, MaBAH1-MaMYB60-CCGs, in controlling chlorophyll catabolism, providing a molecular explanation for green ripening in bananas under high temperatures. This discovery of a chlorophyll degradation regulatory pathway and the underlying molecular elements offer new opportunities for developing technologies for post-harvest fruit and vegetable quality preservation and improvement.

Materials and methods

Plant materials, treatments and growth conditions

Preclimacteric banana (*M. acuminata*, AAA group, cv. Cavendish) fruits at the mature-green stage were obtained from a local commercial plantation near Guangzhou, China. Ripening of bananas was initiated by treatment with 100 μL L^{-1} ethylene for 24 h in an airtight container, and fruits were allowed to ripen at 20 °C or 30 °C (high temperature), as described previously (Wu et al. 2019). Fruits were sampled just before ethylene treatment, which served as the Day 0 samples for both 20 °C and 30 °C treatments. Fruits were sampled, and CI and total chlorophyll content were recorded in 24-h intervals for 6 d of storage following ethylene treatment as described previously (McGuire 1992; Yang et al. 2009).

Nicotiana benthamiana and *A. thaliana* plants used for experiments were planted in commercial potting soil and vermiculite (3:1) within a growth chamber set to 22°C under long-day conditions (16-h light/8-h dark; light intensity 120 to 180 μmol m^{-2} s^{-1}). The leaves of 4- to 6-wk-old *N. benthamiana* plants were selected for Agrobacterium (*Agrobacterium tumefaciens*)-mediated transient overexpression assays.

Gene expression and immunoblot analysis

Total RNA from banana fruit peels and *N. benthamiana* leaves was extracted using the hot borate method (Wan and Wilkins 1994) and a RNeasy Plant Mini Kit

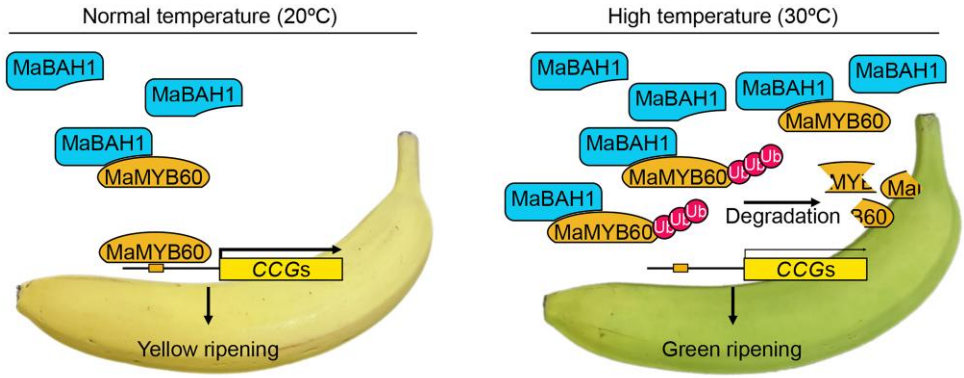

Figure 9. A proposed regulatory network of high temperature-induced repression of chlorophyll catabolism in banana fruit. At 20 °C, MaMYB60 directly targets and activates the expression of CCGs, leading to chlorophyll degradation following normal ripening. Under high temperatures (30 °C), the expression of *MaBAH1* is induced and MaBAH1 accumulates. MaBAH1 promotes the ubiquitination and proteasomal degradation of MaMYB60, which leads to the downregulation of CCGs, thereby repressing chlorophyll degradation in peel and causing green ripening in bananas. Our findings illustrate a dynamic regulatory module of MaBAH1–MaMYB60–CCGs in controlling chlorophyll catabolism during fruit ripening.

(Qiagen, Germany), respectively. First-strand cDNAs were synthesized through reverse transcription using a commercially available TaKaRa PrimeScript RT reagent kit. qPCR was carried out on a Bio-Rad CFX96 Real-Time PCR System using a SYBR Green PCR Supermix Kit (Bio-Rad Laboratories Inc, Dreieich, Germany) following the manufacturer's instructions. Banana *MaACT1* (Chen et al. 2011) and *N. benthamiana EF-1a* (Liu et al. 2012) were used as the reference genes to normalize the transcript levels of target genes in bananas and *N. benthamiana*, respectively.

To produce anti-MaMYB60 and anti-MaBAH1 antibodies, recombinant His-tagged MaMYB60 and MaBAH1 were produced in *Escherichia coli* strain BM Rosetta (DE3), purified using Ni-NTA agarose (GE Healthcare, Buckinghamshire, UK) and used to immunize rabbits. Each polyclonal antibody was affinity-purified from rabbit antisera by Hangzhou HuaAn Biotechnology Co., Ltd (Hangzhou, China). The specificities of the anti-MaMYB60 and anti-MaBAH1 antibodies were validated by immunoblotting analysis using the prokaryote-expressed and purified recombinant protein of GST-MaMYB60 and MBP-MaBAH1, total protein extracts from banana fruit peel, and total protein extracts from *N. benthamiana* leaves overexpressing *MaMYB60* or *MaBAH1* (Supplemental Figs. S17 and S18). Protein from banana fruits was extracted using a protein extraction kit (Bangfei, Beijing, China). Separation of protein (30 μg protein per lane) was performed by SDS–PAGE. After electrophoresis, proteins were electrotransferred onto a nitrocellulose membrane (0.45 μm, Thermo Scientific) using a Bio-Rad transfer apparatus. Immunoblotting analysis was conducted using the anti-MaMYB60 or anti-MaBAH1 antibody, with a secondary goat anti-rabbit IgG peroxidase antibody (Thermo Scientific, cat. no. 32460).

Y1H assay

YIH library screening was performed with the Matchmaker Gold Yeast One-Hybrid System (Clontech, Mountain View, CA). The *MaSGR2* promoter was cloned into the vector pAbAi as the bait. The plasmid was linearized and transformed into Y1H Gold strain to generate the bait-specific reporter strain. Positive yeast strains were then transformed with pGADT7-AD, which contained the banana fruit cDNA library (prey) constructed in our previous study (Shan et al. 2020). Protein–DNA interaction was determined based on the growth of co-transformants on synthetic defined medium lacking Leu (SD/–Leu) containing 300 ng mL^{-1} AbA, according to the manufacturer's protocol.

EMSA

The promoter fragments from CCGs containing MYBRs were synthesized (Sangon Biotech, Shanghai, China) and labeled with biotin at their 5′ end. GST-tagged MaMYB60 was produced in *E. coli* strain BM Rosetta (DE3) and purified with glutathione-Sepharose 4B beads (Takara, cat. no. 635607). EMSA was performed using a LightShift Chemiluminescent EMSA kit (Thermo Scientific, Waltham, MA), as described in our previous reports (Fan et al. 2018; Shan et al. 2020). Briefly, biotin-labeled probes were incubated with recombinant GST-MaMYB60 in binding buffer for 25 min at 22 °C, and the free and bound probes were separated on a native acrylamide gel. Unlabeled probes were used as competitors and GST was used as a negative control.

ChIP-qPCR analysis

ChIP-qPCR analysis was carried out as described in our previous reports (Han et al. 2016; Kuang et al. 2017). Briefly, the banana fruit peels were submerged in 1% (v/v) formaldehyde to crosslink genomic DNA and protein. To extract chromatin, the samples were homogenized in 10 mL extraction buffer 1 (50 mM HEPES-KOH pH 7.5, 1 M sucrose, 5 mM KCl, 5 mM $MgCl_2$, 1 mM EDTA pH 8.0, 1 mM DTT, complete protease inhibitors (Roche, cat. no. 4693132001)). Chromatin was collected by centrifugation for 20 min at 3,500 × *g*, 4 °C and then washed 2 times with 1 mL extraction buffer

2 (10 mM Tris pH 8.0, 1 M sucrose, 5 mM KCl, 5 mM $MgCl_2$, 0.6% [v/v] Triton X-100, 1 mM EDTA, complete protease inhibitors) and 2 times with 300 µL extraction buffer 3 (10 mM Tris pH 8.0, 1 M sucrose, 5 mM KCl, 5 mM $MgCl_2$, 0.1% [v/v] Triton X-100, 1 mM EDTA, complete protease inhibitors). The chromatin was isolated from the ground tissue using nuclei lysis buffer (50 mM Tris pH 8.0, 10 mM EDTA, 1% [w/v] SDS, complete protease inhibitors). Chromatin was sheared to an average length of 500 bp by sonication for 20 cycles (5 s ON and 5 s OFF) at 4 °C. DNA crosslinked to MaMYB60 was immunoprecipitated with the affinity-purified polyclonal antibody against MaMYB60. The distal regions of the CCG promoters containing no MYBRs were used as negative controls.

Dual-luciferase transient expression assay

The promoters of *MaNYC1*, *MaSGR1*, *MaSGR2*, *MaPPH*, and *MaTIC55* were individually cloned into the double-reporter vector pGreenII 0800-LUC, while the full-length *MaMYB60* coding sequence was cloned into the vector pGreenII 62-SK as effector, as described by Hellens et al. (2005). The empty pGreenII 62-SK plasmid was used as a negative control. Agrobacterium strain *EHA105* (pSoup) cultures carrying the resulting effector and reporter plasmids were infiltrated as appropriate pairs into *N. benthamiana* leaves. After 2 d of incubation, absolute LUC and REN activities were measured using a dual-luciferase assay kit (Promega, Madison, WI) on a Luminoskan Ascent Microplate Luminometer (Thermo Scientific) according to the manufacturer's instructions. The transcriptional activation of target promoters was calculated as the ratio of LUC to REN. At least 6 transient assay measurements were included for each pair.

Transient analysis in *N. benthamiana* leaves and banana peel

For *N. benthamiana* leaf transient overexpression studies, the full-length coding sequences of *MaMYB60*, *MaBAH1* or CCGs were cloned individually into the high-level simultaneous expression binary vector pEAQ (Sainsbury et al. 2009). The resulting vectors were subsequently transferred into *N. benthamiana* leaves through Agrobacterium strain EHA105 using the same method as described above in the dual-luciferase assay. Three days after infiltration, *N. benthamiana* leaves were collected for photographic analysis and total chlorophyll content and gene expression quantification.

The experimental procedures for transient overexpression and silencing analysis in banana peel were performed as described in our previous studies (Shan et al. 2020; Zhu et al. 2023). Briefly, the open reading frame of *MaMYB60* and *MaBAH1* were individually cloned in-frame with a 6×His tag sequence (GTGATGGTGATGGTGATG) and cloned into the pCXUN vector harboring the maize (*Zea mays*) *Ubiquitin* promoter (Chen et al. 2009). For the construction of transient virus-induced gene silencing vectors, *MaMYB60* or *MaBAH1* fragments were amplified by PCR using specific primers acquired from the Sol Genomics Network (http://vigs.solgenomics.net/) and cloned into the pTRV2 vector. Agrobacterium strain EHA105 carrying pTRV2-*MaMYB60* or pTRV2-*MaBAH1* together with pTRV1 were mixed at a ratio of 1:1 (Miao et al. 2020) and then injected into mature green banana fruit peel. Transformed fruits were treated with 100 µL L^{-1} ethylene on Day 1 after infiltration and kept at 20 °C or 30 °C for 3 d. The peel around the injection sites was used for the measurement of the CI, chlorophyll content, gene expression, and protein abundance.

IP-MS assay

Banana fruits ripened at 20 °C and 30 °C were treated with 50 µM MG132 (Merck, Darmstadt, Germany) for 16 h before sample collection to stabilize MaMYB60 protein. Proteins were extracted in extraction buffer (50 mM Tris–HCl, pH 7.4, 150 mM NaCl, 2 mM $MgCl_2$, 20% [v/v] glycerol, 5 mM DTT, and 0.1% [v/v] Nonidet P-40) containing a protease inhibitor cocktail (Roche). Cell debris was removed by centrifugation for 10 min at 12,000 × *g*, 4°C. The supernatant was collected and incubated with 10 µL of anti-MaMYB60 antibody at 4 °C overnight. On the second day, 50 µL of protein A agarose beads (Roche) was added. After 4 h of incubation at 4 °C, the beads were centrifuged at 1,000 × *g* at 4°C for 2 min and washed 3 times using washing buffer (50 mM Tris–HCl, pH 7.4, 150 mM NaCl, 2 mM $MgCl_2$, 10% [v/v] glycerol, 5 mM DTT, and 0.1% [v/v] Nonidet P-40). SDS sample buffer (5×) was added to the immunoprecipitated protein complex and proteins were separated by SDS–PAGE. To identify MaMYB60-interacting proteins, protein bands were excised from SDS–PAGE gels and subjected to in-gel trypsin digestion for 8 h at 37 °C with sequencing-grade trypsin (Promega, Madison, WI). Peptides from each gel band were extracted, brought to a final volume of 10 µL with 5% (v/v) formic acid, and analyzed by liquid chromatography tandem mass spectrometry (LC–MS/MS). A nonspecific IgG antibody (Abcam, cat. no. ab205718) served as a negative control to identify nonspecific binding proteins. To verify the MaMYB60–MaBAH1 interaction and the ubiquitination of MaMYB60 in banana fruit, immunoprecipitated proteins were separated by SDS–PAGE, and then subjected to immunoblotting using the following antibodies: anti-MaMYB60 (custom produced by HuaAn Biotechnology), anti-MaBAH1 (custom produced by HuaAn Biotechnology), and anti-ubiquitin (Sigma, cat. no. U119).

Co-IP and ubiquitination assays

Co-IP and ubiquitination assays were also performed in *N. benthamiana* leaves as described earlier (Shan et al. 2020). *MaMYB60-GFP* and *MaBAH1-His* were transiently expressed in *N. benthamiana* leaves by Agrobacterium-mediated transformation. For proteasome inhibition, leaves were infiltrated with 10 µM MG132 solution for 12 h and proteins were then extracted using the method described above in the IP-MS assay. The protein complexes were immunoprecipitated with an anti-GFP antibody and subjected to immunoblotting using anti-His (Abcam, cat. no. ab9108) and anti-GFP (Abcam,

cat. no. ab290) antibodies for the Co-IP assay, and an anti-ubiquitin antibody for the ubiquitination assay.

Y2H, pull-down, co-localization, and split-luciferase assays

Y2H, pull-down, and co-localization assays were performed as described previously (Shan et al. 2020). Briefly, for the Y2H assay, as full-length MaMYB60 showed auto-activation, a truncated fragment of the *MaMYB60* coding sequence encoding the R2R3 domain without auto-activation was cloned into the vector pGBKT7 to yield DB-MaMYB60-R2R3-1.1. Full-length coding sequences of *MaBAH1* and *MaMYB60* were cloned into vectors pGBKT7 and pGADT7 to obtain AD-MaBAH1, or DBD-MaBAH1 and AD-MaMYB60. The appropriate pairs of plasmids were then co-transformed into Y2H Gold yeast cells. The transformed yeast strains were grown at 30 °C on selective medium lacking leucine (Leu), tryptophan (Trp), histidine (His), and adenine (Ade), and the possible protein–protein interactions were evaluated according to their growth status and α-galactosidase activity.

For pull-down assay, recombinant MBP-MaBAH1 was produced in *E. coli* BM Rosetta (DE3) and purified by affinity chromatography using amylose resin (New England Biolabs). GST-MaMYB60 was obtained as described for EMSA. The protein mixtures were captured by a glutathione purification kit (Thermo Fisher Scientific). The eluted proteins were detected using anti-GST (Abcam, cat. no. ab9058) and anti-MBP (Abcam, cat. no. ab9084) antibodies.

For the co-localization assay, the full-length *MaMYB60* and *MaBAH1* coding sequences were cloned into the vectors pEAQ-GFP and pEAQ -mCherry, respectively, and the resulting vectors were co-infiltrated into *N. benthamiana* leaves via Agrobacterium. Two days post-infiltration, GFP and mCherry fluorescence signals were observed with a fluorescence microscope (Zeiss Axio Imager D2) with the GFP filter (excitation/bandpass: 470/40 nm; emission/bandpass: 525/50 nm) and mCherry filter (excitation/bandpass: 550/25 nm; emission/bandpass: 628/40 nm).

For the split-luciferase assay, *MaMYB60* was cloned in-frame and upstream of the sequence encoding the N-terminal half of firefly LUC in pCAMBIA1300-NLUC, while *MaBAH1* was cloned in-frame and downstream of the C-terminal half of luciferase in pCAMBIA1300-CLUC. The resulting vectors, as well as empty plasmids, were introduced into Agrobacterium strain GV3101, and transiently expressed in *N. benthamiana* leaves as described above. Luciferase activity from *N. benthamiana* leaves was detected 3 d after infiltration with a chemiluminescence imager with a cooled charge-coupled device (CCD) camera (Bio-Rad).

In vitro ubiquitination assay

Recombinant GST-MaMYB60 and MBP-MaBAH1 were obtained as described in EMSA and pull-down assay. The ubiquitination assay was performed as described previously (Shan et al. 2020). In brief, recombinant GST-MaMYB60 was incubated with ubiquitin, E1, E2 (Boston Biochem.) and recombinant MBP-MaBAH1, and the reaction products were analyzed by immunoblotting with an anti-GST antibody.

Cell-free degradation assay

MaBAH1-His was transiently expressed in *N. benthamiana* leaf tissue and total proteins were extracted by the same method described in the Co-IP assay procedure. Total protein extracts (50 μg) were incubated with recombinant GST-MaMYB60 for 0, 3 or 6 h at 22 °C. Reactions were terminated by boiling the reaction mixture in SDS sample buffer for 5 min, and then subjected to SDS–PAGE followed by immunoblotting using the anti-GST antibody.

In vivo protein degradation assay

Then the coding region of firefly LUC was amplified from pGreenII 0800-LUC as template and inserted into pEAQ vector, generating pEAQ-LUC. The full-length cDNA of *MaMYB60* was cloned into pEAQ-LUC vector, generating pEAQ-MaMYB60-LUC to express a fusion protein of LUC and MaMYB60. *MaMYB60-LUC* was co-expressed with *MaBAH1* in *N. benthamiana* leaves following Agrobacterium-mediated infiltration. After 48 h, leaves were infiltrated with 10 μM MG132 or distilled water, and incubated for 12 h before harvesting. The proteasome-mediated degradation assay was performed as described by Shan et al. (2020). Total proteins were isolated from transiently infiltrated *N. benthamiana* leaves, and separated by SDS–PAGE, followed by immunoblotting with an anti-LUC antibody (Sigma–Aldrich, cat. no. L0159). LUC activity was measured by the luciferase reporter gene assay, using a commercial kit (Promega Corporation).

Arabidopsis genetic transformation

To overexpress *MaMYB60* or *MaBAH1* in Arabidopsis, their full-length coding sequences were individually cloned into the plant transformation vector pCAMBIA1300-GFP. The resulting plasmids were then introduced into Agrobacterium strain GV3101. WT Columbia (Col-0) Arabidopsis (*A. thaliana*) plants were transformed using the floral dip method (Clough and Bent 1998). Positive transgenic plants were confirmed by immunoblotting with an anti-GFP antibody. For each gene, 3 independent homozygous lines (T3) were used for experiments. Detached rosette leaves of 3-wk-old plants were incubated in complete darkness as described previously (Sakuraba et al. 2014). Photographic analysis, chlorophyll measurement, and gene expression quantification were performed at 0, 3, 5 and 7 d of dark incubation.

PLS-DA

The PLS-DA was used for analyzing the gene expression data as described by Papazian et al. (2016). Quantitative data obtained by RT-qPCR were analyzed by multivariate supervised PLS-DA method with MetaboAnalyst software (https://www.metaboanalyst.ca). The performance of the PLS-DA model was evaluated using the correlation coefficients (R^2) and cross-validation correlation coefficients (Q^2), defining the

proportion of variance in the data explained and predicted by the model, respectively. In each cross-validation step, the expected data were compared to the original data, and the squared sum of errors was calculated. The prediction error was then summed up on all samples (predicted residual sum of squares, PRESS). The PRESS was divided by the initial sum of squares for greater accuracy and subtracted from 1 to resemble the R^2 scale. The 9 CCGs were ranked according to their VIP scores, representing the weighted sums of the PLS-DA weights' squares, indicating the importance of the variable.

Phylogenetic analysis of MYBs

The sequences of MYB proteins from maize and Arabidopsis were retrieved from NCBI database based on previous studies (Kranz et al. 1998; Dubos et al. 2010). The phylogenetic analysis was conducted using the ClustalW. Construction of phylogenic tree using the neighbor-joining method and a bootstrap test of 1,000 replicates was performed with MEGA software. Protein IDs, multiple sequence alignments, and trees in Newick format are available in Supplemental Data Set S2, Supplemental Files S1 and S2, respectively.

Statistical analysis

All experiments were performed at least in triplicate. Statistical analysis was performed with SPSS version 19.0 (SPSS Inc.). Data are shown as means ± standard errors (SE) from 3 or 6 independent biological replicates. Statistical differences between samples were analyzed by Student's *t*-test ($^*P < 0.05$ or $^{**}P < 0.01$). The PLS-DA and the VIP scores were calculated with MetaboAnalyst (https://www.metaboanalyst.ca).

Primers

All primers designed and used in this study are listed in Supplemental Data Set S3.

Accession numbers

Sequence data of all banana genes mentioned in this article can be found in the banana genome database under the following accession numbers: *MaMYB60* (Ma04_g00460.1), *MaBAH1* (Ma05_g02600), *MaNYC1* (Ma07_g10650), *MaPPH* (Ma08_g17060), *MaTIC55* (Ma04_g27140), *MaSGR1* (Ma01_g03010), *MaSGR2* (Ma02_g05320), *MaNOL* (Ma02_g04990), *MaHCAR* (Ma04_g16620), *MaPAO* (Ma04_g31690), and *MaRCCR* (Ma09_g29720). Sequences of *N. benthamiana* genes can be found in the *Nicotiana benthamiana* genome database under the following accession numbers: *NbNYC1* (Nbv6.1trP75488), *NbPPH* (Nbv6.1trP42298), *NbTIC55* (Nbv6.1trP59080), *NbSGR1* (Nbv6.1trP43575), and *NbSGR2* (Nbv6.1trP17492). Sequences of Arabidopsis genes can be found in the NCBI database under the following accession numbers. *AtNYC1* (At4g13250), *AtPPH* (At5g13800), *AtTIC55* (At2g24820), *AtSGR1* (At4g22920), and *AtSGR2* (At4g11910).

Acknowledgments

We would like to thank Dr. George P. Lomonossoff at the John Innes Centre, Norwich Research Park, for the generous gift of pEAQ vectors. We greatly appreciate the suggestions from Prof. Hai-yang Wang (South China Agricultural University) during revision. We thank Charlesworth Author Services (https://www.cwauthors.com/ASPB/) for editing this manuscript. This work was supported by the National Key Research and Development Program of China (grant no. 2022YFD2100101), the National Natural Science Foundation of China (grant no. 32072279), and the China Agriculture Research System of MOF and MARA (grant no. CARS-31).

Author contributions

W.S. and J.-y.C. conceived this project and designed the research. W.W. and W.S. performed most of the experiments. W.W., Y.-y.Y., P.L., J.-f.K., W.-j.L., X.-q.P., J.-y.C., and W.S. analyzed the data. W.W., P.L., J.-y.C., and W.S. wrote and revised the manuscript. J.-f.K., W.-j.L., and X.-q.P. advised on the manuscript. All authors discussed and approved the final manuscript.

Supplemental Data

The following materials are available in the online version of this article.

Supplemental Figure S1. The PLS-DA and the associated VIP scores of CCG expression during banana ripening at 30 °C and 20 °C.

Supplemental Figure S2. Transient overexpression of *MaNYC1*, *MaSGR1*, *MaSGR2*, *MaPPH*, and *MaTIC55* individually in *N. benthamiana* leaves accelerates chlorophyll degradation.

Supplemental Figure S3. Phylogenetic and sequence analysis of MaMYB60.

Supplemental Figure S4. Molecular characterization of MaMYB60.

Supplemental Figure S5. The MYB recognition sequences in the nucleotide sequences of *CCG* promoters.

Supplemental Figure S6. Transient overexpression of *MaMYB60* accelerated chlorophyll degradation in *N. benthamiana* leaves.

Supplemental Figure S7. Overexpression of *MaMYB60* in Arabidopsis accelerates leaf yellowing and senescence.

Supplemental Figure S8. Correlation between MaMYB60 transcription level and CI and chlorophyll content.

Supplemental Figure S9. Correlation between CCG (*MaNYC1*, *MaSGR1*, *MaSGR2*, *MaPPH*, and *MaTIC55*) transcript levels and MaMYB60 transcription and protein levels.

Supplemental Figure S10. Identification of interacting partners of MaMYB60 by IP-MS.

Supplemental Figure S11. Amino acid alignment of MaBAH1 with similar proteins from other plants.

Supplemental Figure S12. E3 ubiquitin ligase activity of MaBAH1.

Supplemental Figure S13. Ripening at 30 °C induces the expression of *MaBAH1*.

Supplemental Figure S14. MaBAH1 attenuates MaMYB60-induced chlorophyll degradation in tobacco leaves.

Supplemental Figure S15. Overexpression of *MaBAH1* in Arabidopsis delays leaf yellowing and senescence.

Supplemental Figure S16. The mRNA and protein levels of MaMYB60 and MaBAH1 in different tissues of banana.

Supplemental Figure S17. Immunoblotting test of anti-MaMYB60 antibody specificity.

Supplemental Figure S18. Immunoblotting test of anti-MaBAH1 antibody specificity.

Supplemental Data Set S1. Identification of MaMYB60-interacting proteins in IP-MS.

Supplemental Data Set S2. Gene codes of R2R3-MYBs used for phylogenetic analysis.

Supplemental Data Set S3. Summary of primers used in this study.

Supplemental Data Set S4. Summary of statistical analyses.

Supplemental File S1. Multiple sequence alignment used for the phylogenetic tree shown in Supplemental Fig. S3A.

Supplemental File S2. Newick format of the phylogenetic tree shown in Supplemental Fig. S3A.

Conflict of interest statement. The authors declare no conflict of interest.

References

Abdelrahman M, El-Sayed M, Jogaiah S, Burritt DJ, Tran LP. The "STAY-GREEN" trait and phytohormone signaling networks in plants under heat stress. Plant Cell Rep. 2017:**36**(7):1009–1025. https://doi.org/10.1007/s00299-017-2119-y

Adato A, Mandel T, Mintz-Oron S, Venger I, Levy D, Yativ M, Dominguez E, Wang Z, de Vos CH, Jetter R, et al. Fruit-surface flavonoid accumulation in tomato is controlled by a slmyb12-regulated transcriptional network. PLoS Genet. 2009:**5**(12):e1000777. https://doi.org/10.1371/journal.pgen.1000777

Agarwal M, Hao Y, Kapoor A, Dong CH, Fujii H, Zheng X, Zhu JK. A R2R3 type MYB transcription factor is involved in the cold regulation of CBF genes and in acquired freezing tolerance. J Biol Chem. 2006:**281**(49):37636–37645. https://doi.org/10.1074/jbc.M605895200

Ampomah-Dwamena C, Thrimawithana AH, Dejnoprat S, Lewis D, Espley RV, Allan AC. A kiwifruit (*Actinidia deliciosa*) R2R3–MYB transcription factor modulates chlorophyll and carotenoid accumulation. New Phytol. 2019:**221**(1):309–325. https://doi.org/10.1111/nph.15362

An JP, Li R, Qu FJ, You CX, Wang XF, Hao YJ. R2R3-MYB transcription factor MdMYB23 is involved in the cold tolerance and proanthocyanidin accumulation in apple. Plant J. 2018:**96**(3):562–577. https://doi.org/10.1111/tpj.14050

An JP, Wang XF, Zhang XW, Xu HF, Bi SQ, You CX, Hao YJ. An apple MYB transcription factor regulates cold tolerance and anthocyanin accumulation and undergoes MIEL1-mediated degradation. Plant Biotechnol J. 2020:**18**(2):337–353. https://doi.org/10.1111/pbi.13201

An JP, Wang XF, Zhang XW, You CX, Hao YJ. Apple B-box protein BBX37 regulates jasmonic acid mediated cold tolerance through the JAZ-BBX37-ICE1-CBF pathway and undergoes MIEL1-mediated ubiquitination and degradation. New Phytol. 2021:**229**(5):2707–2729. https://doi.org/10.1111/nph.17050

Barry CS, McQuinn RP, Chung MY, Besuden A, Giovannoni JJ. Amino acid substitutions in homologs of the STAY-GREEN protein are responsible for the green-flesh and chlorophyll retainer mutations of tomato and pepper. Plant Physiol. 2008:**147**(1):179–187. https://doi.org/10.1104/pp.108.118430

Blackbourn HD, Jeger MJ, John P. Inhibition of degreening in the peel of bananas ripened at tropical temperatures. V. Chlorophyll bleaching activity measured in vitro. Ann Appl Biol. 1990:**117**(1):175–186. https://doi.org/10.1111/j.1744-7348.1990.tb04205.x

Cha KW, Lee YJ, Koh HJ, Lee BM, Nam YW, Paek NC. Isolation, characterization, and mapping of the stay green mutant in rice. Theor Appl Genet. 2002:**104**(4):526–532. https://doi.org/10.1007/s001220100750

Chen S, Songkumarn P, Liu J, Wang GL. A versatile zero background T-vector system for gene cloning and functional genomics. Plant Physiol. 2009:**150**(3):1111–1121. https://doi.org/10.1104/pp.109.137125

Chen L, Zhong HY, Kuang JF, Li JG, Lu WJ, Chen JY. Validation of reference genes for RT-qPCR studies of gene expression in banana fruit under different experimental conditions. Planta. 2011:**234**(2):377–390. https://doi.org/10.1007/s00425-011-1410-3

Chen J, Zhu X, Ren J, Qiu K, Li Z, Xie ZK, Gao J, Zhou X, Kuai BK. Suppressor of overexpression of CO1 negatively regulates dark-induced leaf degreening and senescence by directly repressing pheophytinase and other senescence-associated genes in *Arabidopsis*. Plant Physiol. 2017:**173**(3):1881–1891. https://doi.org/10.1104/pp.16.01457

Christ B, Hauenstein M, Hörtensteiner S. A liquid chromatography-mass spectrometry platform for the analysis of phyllobilins, the major degradation products of chlorophyll in *Arabidopsis thaliana*. Plant J. 2016:**88**(3):505–518. https://doi.org/10.1111/tpj.13253

Clough SJ, Bent AF. Floral dip: a simplified method for Agrobacterium-mediated transformation of Arabidopsis thaliana. Plant J. 1998:**16**(6):735–743. https://doi.org/10.1046/j.1365-313x.1998.00343.x

Cohen E. The effect of temperature and relative humidity during degreening on the colouring of Shamouti orange fruit. J Hortic Sci Biotechnol. 1978:**53**(2):143–146. https://doi.org/10.1080/00221589.1978.11514809

Ding Y, Li H, Zhang X, Xie Q, Gong Z, Yang S. OST1 kinase modulates freezing tolerance by enhancing ICE1 stability in *Arabidopsis*. Dev Cell. 2015:**32**(3):278–289. https://doi.org/10.1016/j.devcel.2014.12.023

Dong CH, Agarwal M, Zhang Y, Xie Q, Zhu JK. The negative regulator of plant cold responses, HOS1, is a RING E3 ligase that mediates the ubiquitination and degradation of ICE1. Proc Natl Acad Sci USA. 2006:**103**(21):8281–8286. https://doi.org/10.1073/pnas.0602874103

Drury R, Hörtensteiner S, Donnison I, Bird CR, Seymour GB. Chlorophyll catabolism and gene expression in the peel of ripening banana fruits. Physiol Plant. 1999:**107**(1):32–38. https://doi.org/10.1034/j.1399-3054.1999.100105.x

Du LN, Song J, Forney C, Palmer LC, Sherry F, Zhang ZQ. Proteome changes in banana fruit peel tissue in response to ethylene and high-temperature treatments. Hortic Res. 2016:**3**:16012. https://doi.org/10.1038/hortres.2016.12

Du LN, Yang XT, Song J, Ma ZZ, Zhang ZQ, Pang XQ. Characterization of the stage dependency of high temperature on green ripening reveals a distinct chlorophyll degradation regulation in banana fruit. Sci Hortic. 2014:**180**:139–146. https://doi.org/10.1016/j.scienta.2014.10.026

Dubos C, Stracke R, Grotewold E, Weisshaar B, Martin C, Lepiniec L. MYB transcription factors in *Arabidopsis*. Trends Plant Sci. 2010:**15**(10):573–581. https://doi.org/10.1016/j.tplants.2010.06.005

Espley RV, Hellens RP, Putterill J, Stevenson DE, Kutty-Amma S, Allan AC. Red colouration in apple fruit is due to the activity of

the MYB transcription factor, MdMYB10. Plant J. 2007:**49**(3): 414–427. https://doi.org/10.1111/j.1365-313X.2006.02964.x

Fan ZQ, Ba LJ, Shan W, Xiao YY, Lu WJ, Kuang JF, Chen JY. A banana R2R3-MYB transcription factor MaMYB3 is involved in fruit ripening through modulation of starch degradation by repressing starch degradation-related genes and MabHLH6. Plant J. 2018:**96**(6): 1191–1205. https://doi.org/10.1111/tpj.14099

Fang C, Li C, Li W, Wang Z, Zhou Z, Shen Y, Wu M, Wu Y, Li G, Kong LA, et al. Concerted evolution of D1 and D2 to regulate chlorophyll degradation in soybean. Plant J. 2014:**77**(5):700–712. https://doi.org/10.1111/tpj.12419

Gao S, Gao J, Zhu XY, Song Y, Li ZP, Ren GD, Zhou X, Kuai BK. ABF2, ABF3, and ABF4 promote ABA-mediated chlorophyll degradation and leaf senescence by transcriptional activation of chlorophyll catabolic genes and senescence-associated genes in *Arabidopsis*. Mol Plant. 2016:**9**(9):1272–1285. https://doi.org/10.1016/j.molp.2016.06.006

Gao Y, Wei W, Zhao X, Tan XL, Fan ZQ, Zhang YP, Jing Y, Meng LH, Zhu BZ, Zhu HL, et al. A NAC transcription factor, NOR-like1, is a new positive regulator of tomato fruit ripening. Hortic Res. 2018:**5**: 75. https://doi.org/10.1038/s41438-018-0111-5

Gous PW, Warren F, Gilbert R, Fox GP. Drought-proofing barley (*Hordeum vulgare*): the effects of stay green on starch and amylose structure. Cereal Chem. 2017:**94**(5):873–880. https://doi.org/10.1094/CCHEM-02-17-0028-R

Guo Y, Cai Z, Gan S. Transcriptome of *Arabidopsis* leaf senescence. Plant Cell Environ. 2004:**27**(5):521–549. https://doi.org/10.1111/j.1365-3040.2003.01158.x

Han YC, Kuang JF, Chen JY, Liu XC, Xiao YY, Fu CC, Wang JN, Wu KQ, Lu WJ. Banana transcription factor MaERF11 recruits histone deacetylase MaHDA1 and represses the expression of MaACO1 and expansins during fruit ripening. Plant Physiol. 2016:**171**(2): 1070–1084. https://doi.org/10.1104/pp.16.00301

Hao D, Jin L, Wen X, Yu F, Xie Q, Guo H. The RING E3 ligase SDIR1 destabilizes EBF1/EBF2 and modulates the ethylene response to ambient temperature fluctuations in *Arabidopsis*. Proc Natl Acad Sci USA. 2021:**118**(6):e2024592118. https://doi.org/10.1073/pnas.2024592118

Hauenstein M, Christ B, Das A, Aubry S, Hörtensteiner S. A role for TIC55 as a hydroxylase of phyllobilins, the products of chlorophyll breakdown during plant senescence. Plant Cell. 2016:**28**(10): 2510–2527. https://doi.org/10.1105/tpc.16.00630

Hellens R, Allan A, Friel E, Bolitho K, Grafton K, Templeton M, Laing W. Transient expression vectors for functional genomics, quantification of promoter activity and RNA silencing in plants. Plant Methods. 2005:**1**(1):13. https://doi.org/10.1186/1746-4811-1-13

Janni M, Gullì M, Maestri E, Marmiroli M, Valliyodan B, Nguyen HT, Marmiroli N. Molecular and genetic bases of heat stress responses in crop plants and breeding for increased resilience and productivity. J Exp Bot. 2020:**71**(13):3780–3802. https://doi.org/10.1093/jxb/eraa034

Jiang S, Chen M, He N, Chen XL, Wang N, Sun QG, Zhang TL, Xu HF, Fang HC, Wang YC, et al. MdGSTF6, activated by MdMYB1, plays an essential role in anthocyanin accumulation in apple. Hortic Res. 2019:**6**(1):40. https://doi.org/10.1038/s41438-019-0118-6

Kamal NM, Alnor Gorafi YS, Abdelrahman M, Abdellatef E, Tsujimoto H. Stay-green trait: a prospective approach for yield potential, and drought and heat stress adaptation in globally important cereals. Int J Mol Sci. 2019:**20**(23):5837. https://doi.org/10.3390/ijms20235837

Kerscher O, Felberbaum R, Hochstrasser M. Modification of proteins by ubiquitin and ubiquitin-like proteins. Ann Rev Cell Dev Biol. 2006:**22**(1):159–180. https://doi.org/10.1146/annurev.cellbio.22.010605.093503

Kim SH, Kim HS, Bahk S, An J, Yoo Y, Kim JY, Chung WS. Phosphorylation of the transcriptional repressor MYB15 by mitogen-activated protein kinase 6 is required for freezing tolerance in *Arabidopsis*. Nucleic Acids Res. 2017:**45**(11):6613–6627. https://doi.org/10.1093/nar/gkx417

Kranz HD, Denekamp M, Greco R, Jin H, Leyva A, Meissner RC, Petroni K, Urzainqui A, Bevan M, Martin C, et al. Towards functional characterisation of the members of the R2R3-MYB gene family from *Arabidopsis thaliana*. Plant J. 1998:**16**(2):263–276. https://doi.org/10.1046/j.1365-313x.1998.00278.x

Kuai BK, Chen JY, Hörtensteiner S. The biochemistry and molecular biology of chlorophyll breakdown. J Exp Bot. 2018:**69**(4):751–767. https://doi.org/10.1093/jxb/erx322

Kuang JF, Chen JY, Liu XC, Han YC, Xiao YY, Shan W, Tang Y, Wu KQ, He JX, Lu WJ. The transcriptional regulatory network mediated by banana (*Musa acuminata*) dehydration-responsive element binding (MaDREB) transcription factors in fruit ripening. New Phytol. 2017:**214**(2):762–781. https://doi.org/10.1111/nph.14389

Lee E, Ahn H, Choe E. Effects of light and lipids on chlorophyll degradation. Food Sci Biotechnol. 2014:**23**(4):1061–1065. https://doi.org/10.1007/s10068-014-0145-x

Lee HG, Seo PJ. The *Arabidopsis* MIEL1 E3 ligase negatively regulates ABA signalling by promoting protein turnover of MYB96. Nat Commun. 2016:**7**(1):12525. https://doi.org/10.1038/ncomms12525

Li YY, Mao K, Zhao C, Zhao XY, Zhang HL, Shu HR, Hao YJ. MdCOP1 ubiquitin E3 ligases interact with MdMYB1 to regulate light-induced anthocyanin biosynthesis and red fruit coloration in apple. Plant Physiol. 2012:**160**(2):1011–1022. https://doi.org/10.1104/pp.112.199703

Li TT, Wu Q, Duan XW, Yun Z, Jiang YM. Proteomic and transcriptomic analysis to unravel the influence of high temperature on banana fruit during postharvest storage. Funct Integr Genomics. 2019b:**19**(3):467–486. https://doi.org/10.1007/s10142-019-00662-7

Li SJ, Xie XL, Liu SC, Chen KS, Yin XR. Auto- and mutual-regulation between two CitERFs contribute to ethylene-induced citrus fruit degreening. Food Chem. 2019a:**299**:125163. https://doi.org/10.1016/j.foodchem.2019.125163

Liu DS, Shi LD, Han CG, Yu JL, Li DW, Zhang YL. Validation of reference genes for gene expression studies in virus-infected *Nicotiana benthamiana* using quantitative real-time PCR. PLoS One. 2012:**7**(9):e46451. https://doi.org/10.1371/journal.pone.0046451

McGuire RG. Reporting of objective color measurements. HortSci. 1992:**27**(12):1254–1255. https://doi.org/10.21273/HORTSCI.27.12.1254

Meguro M, Ito H, Takabayashi A, Tanaka R, Tanaka A. Identification of the 7-hydroxymethyl chlorophyll a reductase of the chlorophyll cycle in *Arabidopsis*. Plant Cell. 2011:**23**(9): 3442–3453. https://doi.org/10.1105/tpc.111.089714

Miao H, Sun P, Liu Q, Liu J, Jia C, Zhao D, Xu B, Jin Z. Molecular identification of the key starch branching enzyme-encoding gene SBE2.3 and its interacting transcription factors in banana fruits. Hortic Res. 2020:**7**(1):101. https://doi.org/10.1038/s41438-020-0325-1

Millard PS, Kragelund BB, Burow M. R2R3 MYB transcription factors-functions outside the DNA-binding domain. Trends Plant Sci. 2019:**24**(10):934–946. https://doi.org/10.1016/j.tplants.2019.07.003

Momose T, Ozeki Y. Regulatory effect of stems on sucrose-induced chlorophyll degradation and anthocyanin synthesis in *Egeria densa* leaves. J Plant Res. 2013:**126**(6):859–867. https://doi.org/10.1007/s10265-013-0581-3

Ogura N, Nakaya H, Takehana H. Studies on the storage temperature of tomato fruit. I. Effect of high temperature-short term storage of mature green tomato fruits on changes of their chemical composition after ripening at room temperature. J Agric Chem Soc Jpn. 1975:**49**(4): 189–196. https://doi.org/10.1271/nogeikagaku1924.49.189

Papazian S, Khaling E, Bonnet C, Lassueur S, Reymond P, Moritz T, Blande JD, Albrectsen BR. Central metabolic responses to ozone and herbivory affect photosynthesis and stomatal closure. Plant Physiol. 2016:**172**(3):2057–2078. https://doi.org/10.1104/pp.16.01318

Prouse MB, Campbell MM. The interaction between MYB proteins and their target DNA binding sites. Biochim Biophys Acta Gene Regul Mech. 2012:**1819**(1):67–77. http://dx.doi.org/10.1016/j.bbagrm.2011.10.010

Pružinská A, Anders I, Tanner G, Roca M, Hörtensteiner S. Chlorophyll breakdown: pheophorbide a oxygenase is a Rieske-type ironsulfur protein, encoded by the accelerated cell death 1 gene. Proc Natl Acad Sci USA. 2003:**100**(25):15259–15264. https://doi.org/10.1073/pnas.2036571100

Qiu K, Li ZP, Yang Z, Chen JY, Wu SX, Zhu XY, Shan G, Gao J, Ren GD, Kuai BK, et al. EIN3 and ORE1 accelerate degreening during ethylene-mediated leaf senescence by directly activating chlorophyll catabolic genes in *Arabidopsis*. PLoS Genet. 2015:**11**(7):e1005399. https://doi.org/10.1371/journal.pgen.1005399

Rampino P, Spano G, Pataleo S, Mita G, Napier JA, di Fonzo N, Shewry PR, Perrotta C. Molecular analysis of a durum wheat 'stay green' mutant: expression pattern of photosynthesis-related genes. J Cereal Sci. 2006:**43**(2):160–168. https://doi.org/10.1016/j.jcs.2005.07.004

Rihani KAL, Jacobsen HJ, Hofmann T, Schwab W, Hassan F. Metabolic engineering of apple by overexpression of the *MdMyb10* gene. J Genet Eng Biotechnol. 2017:**15**(1):263–273. https://doi.org/10.1016/j.jgeb.2017.01.001

Rolando JL, Ramírez DA, Yactayo W, Monneveux P, Quiroz R. Leaf greenness as a drought tolerance related trait in potato (*Solanum tuberosum* L.). Environ Exp Bot. 2015:**110**:27–35. https://doi.org/10.1016/j.envexpbot.2014.09.006

Sainsbury F, Thuenemann EC, Lomonossoff GP. pEAQ: versatile expression vectors for easy and quick transient expression of heterologous proteins in plants. Plant Biotechnol J. 2009:**7**(7):682–693. https://doi.org/10.1111/j.1467-7652.2009.00434.x

Sakuraba Y, Jeong J, Kang MY, Kim J, Paek NC, Choi G. Phytochrome-interacting transcription factors PIF4 and PIF5 induce leaf senescence in Arabidopsis. Nat Commun. 2014:**5**(1):4636. https://doi.org/10.1038/ncomms5636

Santos CV. Regulation of chlorophyll biosynthesis and degradation by salt stress in sunflower leaves. Sci Hortic. 2004:**103**(1):93–99. https://doi.org/10.1016/j.scienta.2004.04.009

Shan W, Kuang JF, Wei W, Fan ZQ, Deng W, Li ZG, Bouzayen M, Pirrello J, Lu WJ, Chen JY. MaXB3 modulates MaNAC2, MaACS1 and MaACO1 stability to repress ethylene biosynthesis during banana fruit ripening. Plant Physiol. 2020:**184**(2):1153–1171. https://doi.org/10.1104/pp.20.00313

Shimoda Y, Ito H, Tanaka A. *Arabidopsis* STAY-GREEN, Mendel's green cotyledon gene, encodes magnesium-dechelatase. Plant Cell. 2016:**28**(9):2147–2160. https://doi.org/10.1105/tpc.16.00428

Thomas H, Howarth CJ. Five ways to stay green. J Exp Bot. 2000:**51**-(suppl_1):329–337. https://doi.org/10.1093/jexbot/51.suppl_1.329

Wan CY, Wilkins TA. A modified hot borate method significantly enhances the yield of high-quality RNA from cotton (*Gossypium hirsutum* L.). Anal Biochem. 1994:**223**(1):7–12. https://doi.org/10.1006/abio.1994.1538

Wang QL, Chen JH, He NY, Guo FQ. Metabolic reprogramming in chloroplasts under heat stress in plants. Int J Mol Sci. 2018:**19**(3):849. https://doi.org/10.3390/ijms19030849

Wang X, Ding YL, Li ZY, Shi YT, Wang JL, Hua J, Gong ZZ, Zhou JM, Yang SH. PUB25 and PUB26 promote plant freezing tolerance by degrading the cold signaling negative regulator MYB15. Dev Cell. 2019:**51**(2):222–235. https://doi.org/10.1016/j.devcel.2019.08.008

Wang X, Niu Y, Zheng Y. Multiple functions of MYB transcription factors in abiotic stress responses. Int J Mol Sci. 2021:**7**(11): 6125. https://doi.org/10.3390/ijms22116125

Wei Y, Jin JT, Xu YX, Liu WT, Yang GX, Bu HD, Li T, Wang AD. Ethylene-activated MdPUB24 mediates ubiquitination of MdBEL7 to promote chlorophyll degradation in apple fruit. Plant J. 2021:**108**(1):169–182. https://doi.org/10.1111/tpj.15432

Wu Q, Ma ZZ, Qin YL, Li YM, Huang BZ, Zhang XL, Du LN, Song J, Zhang ZQ, Pang XQ. Imbalanced expression of *stay-green 1* alleles in banana AAB/ABB cultivars prevents high-temperature-induced green ripening as in AAA Cavendish fruit. Postharvest Biol Technol. 2019:**158**:110980. https://doi.org/10.1016/j.postharvbio.2019.110980

Wu M, Xu X, Hu X, Liu Y, Cao H, Chan H, Gong Z, Yuan Y, Luo Y, Feng B, et al. SlMYB72 regulates the metabolism of chlorophylls, carotenoids, and flavonoids in tomato fruit. Plant Physiol. 2020:**183**(3):854–868. https://doi.org/10.1104/pp.20.00156

Xiang L, Liu X, Li H, Yin X, Grierson D, Li F, Chen K. CmMYB#7, an R3 MYB transcription factor, acts as a negative regulator of anthocyanin biosynthesis in chrysanthemum. J Exp Bot. 2019:**70**(12):3111–3123. https://doi.org/10.1093/jxb/erz121

Xiao YY, Kuang JF, Qi XN, Ye YJ, Wu ZX, Chen JY, Lu WJ. A comprehensive investigation of starch degradation process and identification of a transcriptional activator MabHLH6 during banana fruit ripening. Plant Biotechnol J. 2018:**16**(1):151–164. https://doi.org/10.1111/pbi.12756

Xu WJ, Dubos C, Lepiniec L. Transcriptional control of flavonoid biosynthesis by MYB-bHLH-WDR complexes. Trends Plant Sci. 2015:**20**(3):176–185. https://doi.org/10.1016/j.tplants.2014.12.001

Yang XT, Pang XQ, Xu LY, Fang RQ, Huang XM, Guan PJ, Lu WJ, Zhang ZQ. Accumulation of soluble sugars in peel at high temperature leads to stay-green ripe banana fruit. J Exp Bot. 2009:**60**(14):4051–4062. https://doi.org/10.1093/jxb/erp238

Yin XR, Xie XL, Xia XJ, Yu JQ, Ferguson IB, Giovannoni JJ, Chen KS. Involvement of an ethylene response factor in chlorophyll degradation during citrus fruit degreening. Plant J. 2016:**86**(5):403–412. https://doi.org/10.1111/tpj.13178

Zhang Z, Li J, Li F, Liu H, Yang W, Chong K, Xu Y. OsMAPK3 phosphorylates OsbHLH002/OsICE1 and inhibits its ubiquitination to activate OsTPP1 and enhances rice chilling tolerance. Dev Cell. 2017:**43**(6):731–743. https://doi.org/10.1016/j.devcel.2017.11.016

Zhang J, Yu G, Wen W, Ma X, Xu B, Huang B. Functional characterization and hormonal regulation of the PHEOPHYTINASE gene *LpPPH* controlling leaf senescence in perennial ryegrass. J Exp Bot. 2016:**67**(3):935–945. https://doi.org/10.1093/jxb/erv509

Zhu LS, Chen L, Wu CJ, Shan W, Cai DL, Lin ZX, Wei W, Chen JY, Lu WJ, Kuang JF. Methionine oxidation and reduction of the ethylene signaling component MaEIL9 are involved in banana fruit ripening. J Integr Plant Biol. 2023:**65**(1):150–166. https://doi.org/10.1111/jipb.13363

Zhu M, Chen G, Zhou S, Tu Y, Wang Y, Dong T, Hu Z. A new tomato NAC (NAM/ATAF1/2/CUC2) transcription factor, SlNAC4, functions as a positive regulator of fruit ripening and carotenoid accumulation. Plant Cell Physiol. 2014:**55**(1):119–135. https://doi.org/10.1093/pcp/pct162

Zhu F, Luo T, Liu C, Wang Y, Yang H, Yang W, Zheng L, Xiao X, Zhang M, Xu R, et al. An R2R3-MYB transcription factor represses the transformation of α- and β-branch carotenoids by negatively regulating expression of *CrBCH2* and *CrNCED5* in flavedo of *Citrus reticulate*. New Phytol. 2017:**216**(1):178–192. https://doi.org/10.1111/nph.14684